

Unveiling the Strong Interaction origin of Baryon Masses with Lattice QCD (CLQCD Collaboration)



Bolun Hu,¹ Haiyang Du,^{2,1} Xiangyu Jiang,¹ Keh-Fei Liu,^{3,4} Peng Sun,⁵ and Yi-Bo Yang^{1,2,6,7,*}

¹*CAS Key Laboratory of Theoretical Physics, Institute of Theoretical Physics,
Chinese Academy of Sciences, Beijing 100190, China*

²*University of Chinese Academy of Sciences, School of Physical Sciences, Beijing 100049, China*

³*University of Kentucky, Lexington, KY 40506, USA*

⁴*Nuclear Science Division, Lawrence Berkeley National Laboratory, Berkeley, California 94720, USA*

⁵*Institute of Modern Physics, Chinese Academy of Sciences, Lanzhou, 730000, China*

⁶*School of Fundamental Physics and Mathematical Sciences,*

Hangzhou Institute for Advanced Study, UCAS, Hangzhou 310024, China

⁷*International Centre for Theoretical Physics Asia-Pacific, Beijing/Hangzhou, China*

(Dated: May 6, 2025)

Both the Higgs mechanism and strong interactions contribute to the masses of visible matter, yet how the six Higgs-generated quark masses and uniform strong interaction strength determine the hundreds of hadron masses remains unclear. Additionally, the role of massless, flavor-neutral gluons on hadron mass formation is central to the unresolved Millennium Prize problem on the mass gap in Yang-Mills theory. Addressing these questions requires advanced simulations on state-of-the-art supercomputers using Lattice Quantum Chromodynamics (QCD), which offers a rigorous, non-perturbative definition of QCD solvable numerically [1]. Here we present first-principles lattice QCD calculations using comprehensive gauge ensembles [2, 3] that accurately predict ground state spin-1/2 and spin-3/2 baryon masses with light, strange, and charm quarks within 1% of experimental values. At the $\overline{\text{MS}}$ 2 GeV scale, our results unveil two fundamental mass generation mechanisms for those baryon masses in QCD: 1) the flavor-dependent enhancement of Higgs contributions, 4-8 for light, 2-3 for strange, and 1.2-1.3 for charm quarks; and 2) the flavor-insensitive contribution 0.8-1.2 GeV from gluon quantum anomaly [4-6]. This breakthrough significantly advances our comprehension of strong interaction dynamics and the genesis of visible matter's mass.

Visible matter in the universe is composed of fundamental particles of the Standard Model (SM) of particle physics. During the first 10^{-11} seconds after the Big Bang, all fundamental particles in SM are massless, leading to a state of nearly scale invariance in the universe. Following this period, the Higgs mechanism spontaneously breaks scale invariance and provides mass to these fundamental particles, resulting in the heaviest quark being approximately 10^5 times more massive than the lightest one. However, a second instance of spontaneous scale invariance breaking occurs at a relatively later stage like 10^{-5} seconds in the universe, becoming an even more significant source of mass for visible matter, overshadowing the contribution of the Higgs mechanism.

This additional source of mass arises from the strong interaction between quarks and gluons, which is described by quantum chromodynamics (QCD) through the

following Lagrangian:

$$\mathcal{L} = -\frac{1}{2}\text{Tr}G_\mu G^\mu + \sum_q \bar{q}(\gamma_\mu(\partial^\mu + igB^\mu) + m_q)q, \quad (1)$$

where $G_{\mu\nu} = \partial_\mu B_\nu - \partial_\nu B_\mu + g[B_\mu, B_\nu]$, with B_μ representing a 3×3 Hermitian matrix field that interacts with itself via the QCD coupling constant g . The matrices γ_μ are the Dirac matrices, and different quark “flavors” are depicted by distinct fermionic fields q with masses m_q , which can be interpreted as the effective coupling between quarks and the Higgs boson.

The contribution from the Higgs mechanism to the mass of hadrons (such as protons and neutrons, which predominantly interact via strong forces) through a given quark flavor q can be expressed as $\sigma_{q,H} \equiv m_q \langle \bar{q}q \rangle_H$, where $\langle \bar{q}q \rangle_H$ with $\langle O \rangle_H \equiv \langle H|O|H \rangle / \langle H|H \rangle$ can be understood as the condensate of quark and anti-quark within the hadron H .

Furthermore, quantum corrections in QCD cause both the gauge coupling g and the quark mass m_q to increase at longer distance scales, resulting in an additional breaking of scale invariance. Consequently, the

* Corresponding author: ybyang@itp.ac.cn

energy-momentum tensor of matter, which couples matter to gravity, exhibits a non-vanishing trace, even as m_q approaches zero—this phenomenon is referred to as the “trace anomaly”.

By combining sigma terms and the trace anomaly, one can decompose the total hadron mass as [4–6],

$$m_H = \sum_q \sigma_{q,H} + \gamma_m \sum_q \sigma_{q,H} + \frac{\beta(\alpha_s)}{2\alpha_s} \langle G^{\mu\nu} G_{\mu\nu} \rangle_H, \quad (2)$$

where m_H is the hadron mass, $\gamma_m = \frac{2}{\pi}\alpha_s + \mathcal{O}(\alpha_s^2)$ is the scale violation of quark mass anomalous dimension with $\alpha_s = \frac{g^2}{4\pi}$, and $\frac{\beta(\alpha_s)}{2\alpha_s} = (-\frac{11}{8\pi} + \frac{N_f}{12\pi})\alpha_s + \mathcal{O}(\alpha_s^2)$ is that of the effective strong coupling constant α_s with N_f being the number of quark flavors. Thus, the quark trace anomaly term γ_m enhances the quark sigma term contri-

bution by an $\mathcal{O}(\alpha_s)$ correction, while the remaining part, associated with the gluon trace anomaly, is suppressed by an additional $\mathcal{O}(\alpha_s)$ factor in its contribution to the hadron mass via the double gluon exchange diagram. Additionally, there exist decompositions of the hadron rest energy, as discussed in Refs. [7–10].

Since α_s is of order $\mathcal{O}(1)$ at the scale of the proton charge radius, the QCD interactions become strongly non-linear, potentially causing the power counting of α_s to break down. Ab initio calculations using a discretized Lagrangian on a hyper-cubic spacetime lattice, characterized by a finite lattice spacing a and a spatial size L , transform QCD into a four-dimensional statistical physics system, lattice QCD [1]. These calculations can precisely determine hadron masses and contributions from various sources through importance sampling [11]. The physical predictions are realized by taking the limits as $a \rightarrow 0$ and $L \rightarrow \infty$.

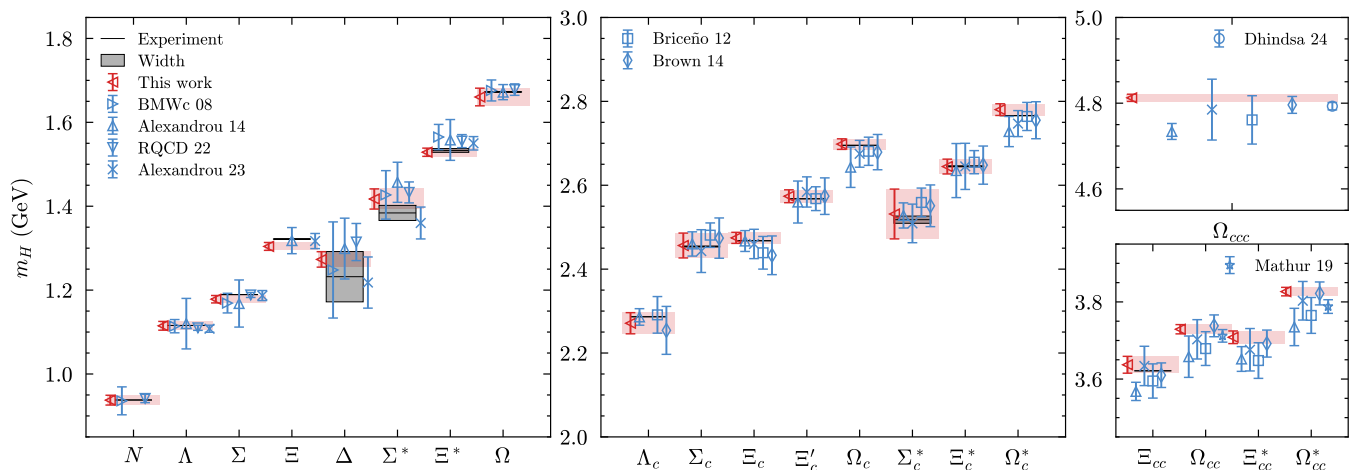


FIG. 1. **Comparison of Lattice QCD Baryon mass prediction and experimental values.** Red triangles and the accompanying red band represent our results, which are compared to previous studies (BMW 08 [12], Alexandrou 14 [13], RQCD 22 [14] Alexandrou 23 [15], Briceno 12 [16], Brown 14 [17], Mathur 19 [18], and Dhindsa 24 [19]) extrapolated to the continuum and physical quark masses. Experimental values are shown as black lines with shaded bands indicating decay widths. The figure consists of four panels, each corresponding to baryons containing 0 (left), 1 (middle), 2 (lower right), and 3 (upper right) charm quarks, respectively. In most cases, our predictions achieve the highest precision to date and exhibit good agreement with experimental values.

Based on the calculation with strange quark and two degenerated light quarks using 23,845 (for the proton and Δ baryon) and 17,725 (for the other baryons) measurements on the 3,340 configurations of 14 ensembles [2, 3] in total, we predict the masses of $J^P = \frac{1}{2}^+$ and $\frac{3}{2}^+$ ground state baryons, and compare the results (red triangles and bands) with those in the literature [12, 13, 16, 17, 19] (blue data points) and available experimental data (black lines with shaded bands indicating decay widths to account for resonance effects in the measurements [12]), in Fig. 1. There are also several lattice results without

the continuum extrapolation which are not illustrated here [20–26]. The black bands and blue data points are omitted where data are unavailable. This analysis includes baryons ranging from light to singly, doubly, and triply charmed species. In most cases, our predictions achieve the highest precision to date and exhibit good agreement with experimental values.

Accurate lattice QCD prediction requires good control on kinds of systematic uncertainties, as we address below:

1) Mismatch effects arising from the masses of the light and strange quarks: The ensembles [2, 3] use different

light quark masses ranging from 0.8 to 6.7 times the averaged mass of the up and down quarks. This allows us to interpolate the light quark mass to its physical value, using the SU(4|2) partially quenched heavy baryon chiral perturbation theory (χ PT) ansatz [8, 27] for the light baryons N and Δ , along with linear interpolation for the other baryons. Furthermore, we adjust the mass of the valence strange quark used to construct the baryon field to its physical value for each ensemble. By performing a joint fit across all the ensembles, we effectively eliminate the mismatch effects from the light and strange quarks loops.

2) Impact of tuning the charm quark mass and considering the missing charm quark loop: Similar to our approach with the strange quark, we adjust the valence charm quark mass to correspond with the physical mass of the D_s meson in each ensemble, and then eliminate the mismatch effects from the light and strange quark loops through a joint fit. As demonstrated in the newest review from Flavor lattice average group (FLAG) [28], which averages the lattice results from independent computations, the outcomes with and without the charm quark loop effects are consistent within the uncertainties. Notably, our prediction for $m_{\Omega_{ccc}}$ aligns with that of Dhindsa 24 [19], which included the charm quark loop in their calculations using different discretizations and also extrapolated to the continuum limit as $a \rightarrow 0$, similar to our calculation here.

3) Continuum and infinite volume extrapolation: We find that the linear a^2 correction adequately describes the masses of baryons without the charm quark across different lattice spacings a . Additionally, the a^4 correction is crucial for capturing the a dependence of certain charmed baryons. Consequently, we retain the a^4 term in the continuum extrapolation for all charmed baryons, which results in our predictions exhibiting relatively larger uncertainties compared to some cases without valence charm quark. We also include the leading-order finite volume correction in our fit, and its impact is shown to be smaller than the statistical uncertainties.

4) Isospin symmetry breaking (ISB) and quantum electrodynamics (QED) effects: Naive power counting indicates that both effects are at the 1% level and then unlikely to alter the conclusions presented in this work. Therefore, we defer their investigation to future studies.

More evidence validating above procedure are provided in the supplementary information.

The scalar matrix elements (ME) $\langle \bar{q}q \rangle_H$ can be obtained from the quark mass dependence of the hadron mass via the Feynman-Hellman theorem [8, 13, 14, 29–46], or direct calculation of the scalar operator $\bar{q}q$ ME in the hadron state H [47–53]. Since the consistency of the two strategies has been validated for both light and charm quarks in the CLQCD ensembles after performing the continuum extrapolation [2, 3], we opt for the Feynman-Hellman theorem, which avoids the complications associated with the direct ME calculation. The consistency of the light quark matrix element in the octet

light baryon using two approaches is also verified using different fermion discretizations [8, 54].

The combined contribution $\sigma_H \equiv \sum_q \sigma_{q,H}$ of all the quark flavors in the nucleon case corresponds to the effective Higgs-nucleon couplings [55, 56], and is crucial for constraining dark matter-nucleon interactions in direct detection experiments [57, 58]. After σ_H is obtained, the trace anomaly contribution and its glue part can be extracted from Eq. (2),

$$\begin{aligned} \langle H_a \rangle_H &= m_H^{\text{phys}} - \sigma_H, \\ \langle H_a^g \rangle_H &= \langle H_a \rangle_H - \gamma_m \sigma_H = m_H^{\text{phys}} - (1 + \gamma_m) \sigma_H. \end{aligned} \quad (3)$$

1) Light quark sigma term $\sigma_{\pi H} \equiv \sigma_{uH} + \sigma_{dH}$: The upper left panel of Fig. 2 displays the light quark σ terms, representing the direct contributions of light quark masses to the baryon mass. Some of the enhancement originates solely from the light quark loop (a gluon splits into a quark and anti-quark pair which combines into another gluon at a later time), as observed in the cases of $\Omega_{(c/cc/cc)}^{(*)}$ baryons (gray triangles), which do not have any valence light quark. However, the $\sigma_{\pi H}$ of other baryons can be significantly larger, as $\langle \bar{q}q \rangle_H$ of the valence quark can be about four times greater than the number of valence light quarks, using the average up and down quark mass of 3.39(4) MeV at $\overline{\text{MS}} 2$ GeV [28, 59–64]. This additional enhancement is likely associated with the connected-sea mechanism [65], where a gluon can split into a quark that moves forward in time and an antiquark that combines with a quark from the past to form another gluon, thereby introducing a surplus of quarks and antiquarks. In terms of the Feynman diagram, this mechanism is akin to a scenario where a valence light quark travels back in time and returns due to interactions with the gluon.

2) Strange quark sigma term σ_{sH} : When the quark mass reaches the magnitude of the strange quark mass 92.4(1.0) MeV at $\overline{\text{MS}} 2$ GeV [28, 59–63, 66], the enhancements from both the quark loop and connected-sea mechanisms diminish, as the gluon must provide significantly more energy for the related processes to occur. Consequently, as observed in the upper-right panel of Fig. 2, the enhancement factor decreases to approximately 1.5, regardless of the number of valence strange quarks, angular momentum, or the flavor of the remaining quarks. This factor is considerably smaller compared to that of the light quark, indicating that the strange quark exhibits less relativistic behavior.

3) Charm quark sigma term σ_{cH} : The lower-left panel of Fig. 2 illustrates that the charm quark scenario is notably more consistent, with the valence σ_{cH} being directly proportional to the charm quark by a factor of approximately 1. In comparison to the charm quark mass of 1.093(7) GeV at $\overline{\text{MS}} 2$ GeV [28, 63, 67–71], the ratio may be slightly smaller than the number of valence charm quark masses. Since the quark mass decreases at higher energy scales, this suggests that an inherent scale—required to ensure that $\langle \bar{c}c \rangle$ matches the number

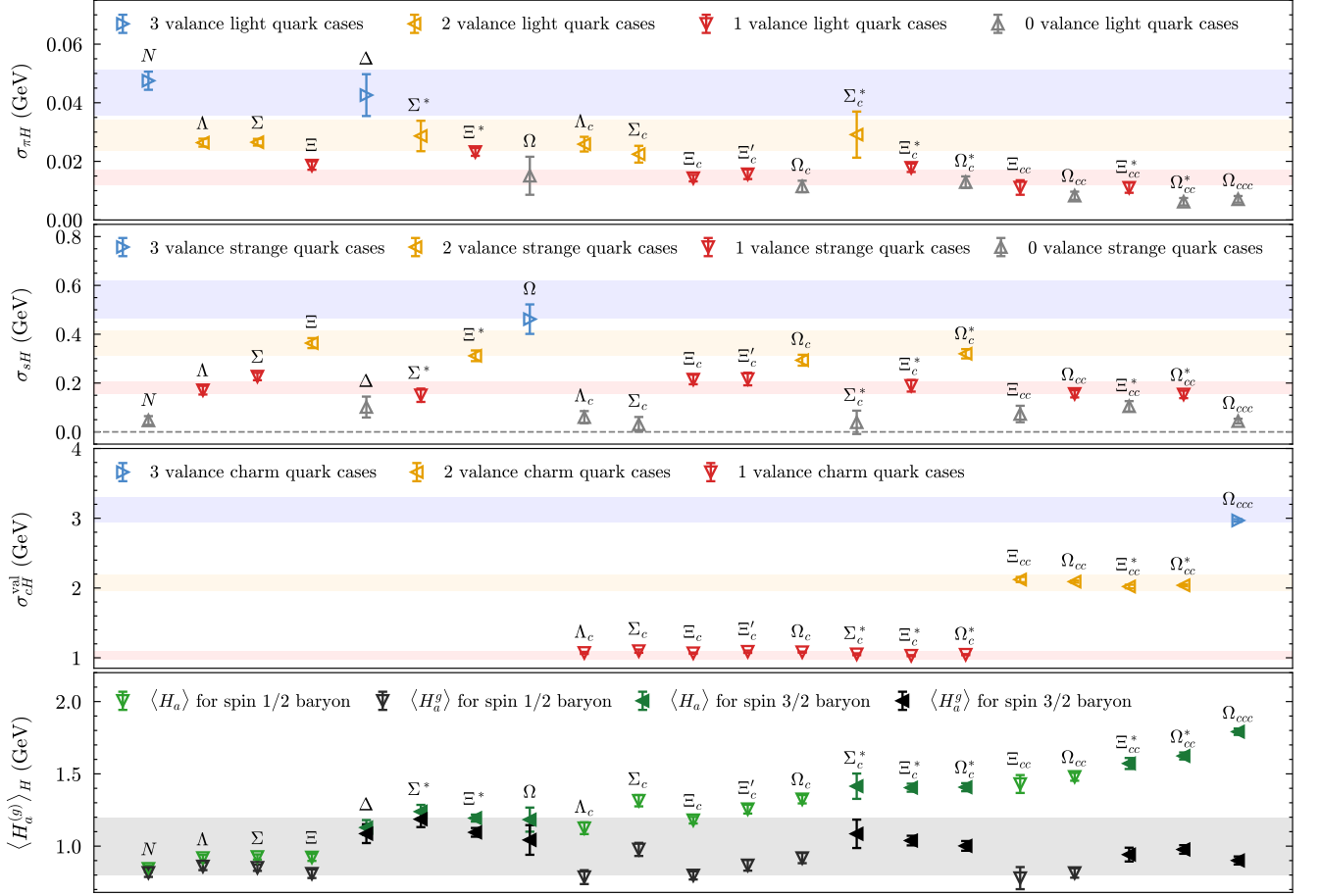


FIG. 2. **Quark sigma terms and trace anomaly contributions to baryon masses.** The top, middle-upper and middle-lower panels show the σ terms for light, strange, and charm quarks, respectively, with colors indicating the number of valence quarks: gray (0), red (1), yellow (2), and blue (3). Most colored data points align with their corresponding colored bands, following the scaling law based on quark numbers. The bottom panel presents the trace anomaly $\langle H_a \rangle_H$ (green triangles) and the gluon trace anomaly $\langle H_a^g \rangle_H$ (black ones), with hollow triangles for spin-1/2 baryons and filled triangles for spin-3/2 baryons. A gray band indicates the range of $\langle H_a^g \rangle_H$ values for all displayed baryons.

of valence charm quarks—must be higher as the number of valence charm quarks increases. This scale ultimately reaches 2.9 GeV for the heaviest Ω_{ccc} , which contains three valence charm quarks.

The charm sea quark contribution to the baryon mass is neglected here, not only because our gauge ensemble includes only light and strange quarks, but also due to the heavy quark relation $m_Q \bar{Q}Q = -\frac{\alpha_s}{12\pi} F^2$ [6, 72], which implies that the heavy sea quark contribution is canceled by the N_f dependence of the gluon trace anomaly at leading order, leading to the decoupling theorem [73]. One can also calculate this contribution based on the trace anomaly, as discussed below.

4) Trace anomaly contribution: By subtracting the total σ term from the baryon mass using Eq. (3), the values of $\langle H_a \rangle_H$ (represented by hollow triangles) for different hadrons H are displayed in the lower-right panel of Fig. 2. It is evident that $\langle H_a \rangle_H$ increases with the number of heavy valence quarks, resulting in a twofold

enhancement from the lightest baryon $\langle H_a \rangle_N$ to the heaviest one $\langle H_a \rangle_{\Omega_{ccc}}$ that we have examined. However, what is particularly noteworthy is that $\langle H_a^g \rangle_H$ (depicted by filled triangles) becomes less dependent on the valence flavor composition and converges around 1 GeV when we further subtract the anomalous sigma term $\gamma_m \sigma_H$ with $\gamma_m = 0.295$ at $\overline{\text{MS}}$ 2 GeV [74]. Interestingly, the spin-3/2 baryons exhibit slightly higher gluon trace anomaly contributions compared to their spin-1/2 counterparts.

Based on the relation $m_Q \bar{Q}Q = -\frac{\alpha_s}{12\pi} F^2$, one can estimate the heavy sea quark contribution to all kinds of the baryon we studied here to be 74(15) MeV at the leading order of the strong coupling and consistent with the direct calculations using gauge ensembles including a dynamical heavy quark [30].

More details of the $\sigma_{q,H}$ calculation can also be found in the supplemental information.

In summary, the ground state masses of $\frac{1}{2}^+$ and $\frac{3}{2}^+$ baryons with the lightest four flavors are predicted by ef-

fectively controlling all systematic uncertainties, except for the ISB and QED effects, along with the contributions from Higgs and gluon couplings of the quarks. Despite the Higgs coupling to the charm quark is hundreds of times that of the light quark, its impact on visible matter is largely disregarded when the valence heavy quark in the baryon decays to the light quark through weak interactions. In contrast, the baryon mass resulting from the gluon trace anomaly persists. Consequently, the gluon trace anomaly, which is insensitive to hadrons, along with the heavy quark loop contribution which is proportional to the gluon trace anomaly one and insensitive to the Higgs coupling, emerges as the primary source of visible matter. Furthermore, the strong interaction also mitigates the Higgs coupling to the baryon through various quark flavors, exhibiting a more substantial enhancement for lighter quarks.

Recent direct calculations of the gluon trace anomaly contribution [75] reveal that this contribution is significantly smaller for the pion—QCD’s pseudo-Goldstone boson—and vanishes in the limit of negligible quark masses. Complementary studies of the pion’s spatial distribution [75] and form factors [76, 77] further suggest the presence of a negative mass “hollow” at its center, arising from the trace anomaly. This distinctive feature differentiates the pion’s mass structure from that of other hadrons. Insights into these phenomena can be indirectly derived through the off-diagonal components of the energy-momentum tensor (EMT) form factors [78, 79], guided by EMT sum rules [10, 80], and may also be probed experimentally via near-threshold J/Ψ photoproduction [81–83]. These findings highlight the need for

deeper exploration to elucidate the unique mechanisms by which strong interactions govern the origin of visible mass in hadronic systems.

ACKNOWLEDGMENT

We thank the CLQCD collaborations for providing us their gauge configurations with dynamical fermions [2], which are generated on HPC Cluster of ITP-CAS, the Southern Nuclear Science Computing Center(SNSC) and the Siyuan-1 cluster supported by the Center for High Performance Computing at Shanghai Jiao Tong University. We thank Hanyang Xing for providing two-point functions using distillation method for comparison, and Gunnar Bali, Ying Chen, Hengtong Ding, Xu Feng, Jianxiao Gong, Chuan Liu, Liuming Liu, Zhaofeng Liu, Ji-Hao Wang, Kuan Zhang, and the other CLQCD members for valuable comments and suggestions. The calculations were performed using PyQUDA [84] and Chroma [85] with QUDA [86–88], through HIP programming model [89]. The numerical calculation were carried out on the ORISE Supercomputer, HPC Cluster of ITP-CAS and Advanced Computing East China Sub-center. This work is supported in part by National Key R&D Program of China No.2024YFE0109800, NSFC grants No. 12293060, 12293062, 12435002, 12293065 and 12047503, the Strategic Priority Research Program of Chinese Academy of Sciences, Grant No. XDB34030303 and YSBR-101, and also the science and education integration young faculty project of University of Chinese Academy of Sciences.

-
- [1] K. G. Wilson, *Phys. Rev. D* **10**, 2445 (1974).
 - [2] Z.-C. Hu *et al.* (CLQCD), *Phys. Rev. D* **109**, 054507 (2024), [arXiv:2310.00814 \[hep-lat\]](#).
 - [3] H.-Y. Du *et al.* (CLQCD), (2024), [arXiv:2408.03548 \[hep-lat\]](#).
 - [4] J. C. Collins, A. Duncan, and S. D. Joglekar, *Phys. Rev. D* **16**, 438 (1977).
 - [5] N. K. Nielsen, *Nucl. Phys. B* **120**, 212 (1977).
 - [6] M. A. Shifman, A. I. Vainshtein, and V. I. Zakharov, *Phys. Lett.* **B78**, 443 (1978).
 - [7] X.-D. Ji, *Phys. Rev. Lett.* **74**, 1071 (1995), [arXiv:hep-ph/9410274](#).
 - [8] Y.-B. Yang, J. Liang, Y.-J. Bi, Y. Chen, T. Draper, K.-F. Liu, and Z. Liu, *Phys. Rev. Lett.* **121**, 212001 (2018), [arXiv:1808.08677 \[hep-lat\]](#).
 - [9] C. Lorcé, H. Moutarde, and A. P. Trawiński, *Eur. Phys. J. C* **79**, 89 (2019), [arXiv:1810.09837 \[hep-ph\]](#).
 - [10] K.-F. Liu, *Phys. Lett. B* **849**, 138418 (2024), [arXiv:2302.11600 \[hep-ph\]](#).
 - [11] S. Duane, A. D. Kennedy, B. J. Pendleton, and D. Roweth, *Phys. Lett. B* **195**, 216 (1987).
 - [12] S. Durr *et al.* (BMW), *Science* **322**, 1224 (2008), [arXiv:0906.3599 \[hep-lat\]](#).
 - [13] C. Alexandrou, V. Drach, K. Jansen, C. Kallidonis, and G. Koutsou, *Phys. Rev. D* **90**, 074501 (2014), [arXiv:1406.4310 \[hep-lat\]](#).
 - [14] G. S. Bali, S. Collins, P. Georg, D. Jenkins, P. Korcyl, A. Schäfer, E. E. Scholz, J. Simeth, W. Söldner, and S. Weishäupl (RQCD), *JHEP* **05**, 035 (2023), [arXiv:2211.03744 \[hep-lat\]](#).
 - [15] C. Alexandrou, S. Bacchio, G. Christou, and J. Finkenrath, *Phys. Rev. D* **108**, 094510 (2023), [arXiv:2309.04401 \[hep-lat\]](#).
 - [16] R. A. Briceño, H.-W. Lin, and D. R. Bolton, *Phys. Rev. D* **86**, 094504 (2012), [arXiv:1207.3536 \[hep-lat\]](#).
 - [17] Z. S. Brown, W. Detmold, S. Meinel, and K. Orginos, *Phys. Rev. D* **90**, 094507 (2014), [arXiv:1409.0497 \[hep-lat\]](#).
 - [18] N. Mathur and M. Padmanath, *Phys. Rev. D* **99**, 031501 (2019), [arXiv:1807.00174 \[hep-lat\]](#).
 - [19] N. S. Dhindsa, D. Chakraborty, A. Radhakrishnan, N. Mathur, and M. Padmanath, (2024), [arXiv:2411.12729 \[hep-lat\]](#).
 - [20] S. Aoki *et al.* (PACS-CS), *Phys. Rev. D* **79**, 034503 (2009), [arXiv:0807.1661 \[hep-lat\]](#).
 - [21] W. Bietenholz *et al.*, *Phys. Rev. D* **84**, 054509 (2011), [arXiv:1102.5300 \[hep-lat\]](#).

- [22] C. Alexandrou and C. Kallidonis, *Phys. Rev. D* **96**, 034511 (2017), [arXiv:1704.02647 \[hep-lat\]](#).
- [23] L. Liu, H.-W. Lin, K. Orginos, and A. Walker-Loud, *Phys. Rev. D* **81**, 094505 (2010), [arXiv:0909.3294 \[hep-lat\]](#).
- [24] Y. Namekawa *et al.* (PACS-CS), *Phys. Rev. D* **87**, 094512 (2013), [arXiv:1301.4743 \[hep-lat\]](#).
- [25] P. Pérez-Rubio, S. Collins, and G. S. Bali, *Phys. Rev. D* **92**, 034504 (2015), [arXiv:1503.08440 \[hep-lat\]](#).
- [26] J.-B. Li, L.-C. Gui, W. Sun, J. Liang, and W. Qin, (2022), [arXiv:2211.04713 \[hep-lat\]](#).
- [27] B. C. Tiburzi, *Phys. Rev. D* **72**, 094501 (2005), [Erratum: *Phys.Rev.D* 79, 039904 (2009)], [arXiv:hep-lat/0508019](#).
- [28] Y. Aoki *et al.* (Flavour Lattice Averaging Group (FLAG)), (2024), [arXiv:2411.04268 \[hep-lat\]](#).
- [29] A. Agadjanov, D. Djukanovic, G. von Hippel, H. B. Meyer, K. Ottnad, and H. Wittig, *Phys. Rev. Lett.* **131**, 261902 (2023), [arXiv:2303.08741 \[hep-lat\]](#).
- [30] S. Borsanyi, Z. Fodor, C. Hoelbling, L. Lellouch, K. K. Szabo, C. Torrero, and L. Varnhorst, (2020), [arXiv:2007.03319 \[hep-lat\]](#).
- [31] P. M. Copeland, C.-R. Ji, and W. Melnitchouk, *Phys. Rev. D* **107**, 094041 (2023), [arXiv:2112.03198 \[nucl-th\]](#).
- [32] M. Frink and U.-G. Meissner, *JHEP* **07**, 028 (2004), [arXiv:hep-lat/0404018](#).
- [33] R. Gupta, S. Park, M. Hoferichter, E. Mereghetti, B. Yoon, and T. Bhattacharya, *Phys. Rev. Lett.* **127**, 242002 (2021), [arXiv:2105.12095 \[hep-lat\]](#).
- [34] J. Martin Camalich, L. S. Geng, and M. J. Vicente Vacas, *Phys. Rev. D* **82**, 074504 (2010), [arXiv:1003.1929 \[hep-lat\]](#).
- [35] K. I. Ishikawa *et al.* (PACS-CS), *Phys. Rev. D* **80**, 054502 (2009), [arXiv:0905.0962 \[hep-lat\]](#).
- [36] X.-L. Ren, L.-S. Geng, and J. Meng, *Phys. Rev. D* **91**, 051502 (2015), [arXiv:1404.4799 \[hep-ph\]](#).
- [37] X. L. Ren, L. S. Geng, J. Martin Camalich, J. Meng, and H. Toki, *JHEP* **12**, 073 (2012), [arXiv:1209.3641 \[nucl-th\]](#).
- [38] A. Semke and M. F. M. Lutz, *Phys. Lett. B* **717**, 242 (2012), [arXiv:1202.3556 \[hep-ph\]](#).
- [39] R. D. Young and A. W. Thomas, *Nucl. Phys. A* **844**, 266C (2010), [arXiv:0911.1757 \[hep-lat\]](#).
- [40] L. Alvarez-Ruso, T. Ledwig, J. Martin Camalich, and M. J. Vicente-Vacas, *Phys. Rev. D* **88**, 054507 (2013), [arXiv:1304.0483 \[hep-ph\]](#).
- [41] S. Durr *et al.* (BMW), *Phys. Rev. D* **85**, 014509 (2012), [Erratum: *Phys.Rev.D* 93, 039905 (2016)], [arXiv:1109.4265 \[hep-lat\]](#).
- [42] R. Horsley, Y. Nakamura, H. Perlt, D. Pleiter, P. E. L. Rakow, G. Schierholz, A. Schiller, H. Stuben, F. Winter, and J. M. Zanotti (QCDSF-UKQCD), *Phys. Rev. D* **85**, 034506 (2012), [arXiv:1110.4971 \[hep-lat\]](#).
- [43] C. S. An and B. Sanghai, *Phys. Rev. D* **92**, 014002 (2015), [arXiv:1404.2389 \[hep-ph\]](#).
- [44] P. Junnarkar and A. Walker-Loud, *Phys. Rev. D* **87**, 114510 (2013), [arXiv:1301.1114 \[hep-lat\]](#).
- [45] K. Takeda, S. Aoki, S. Hashimoto, T. Kaneko, J. Noaki, and T. Onogi (JLQCD), *Phys. Rev. D* **83**, 114506 (2011), [arXiv:1011.1964 \[hep-lat\]](#).
- [46] D. Toussaint and W. Freeman (MILC), *Phys. Rev. Lett.* **103**, 122002 (2009), [arXiv:0905.2432 \[hep-lat\]](#).
- [47] C. Alexandrou, S. Bacchio, M. Constantinou, J. Finkenrath, K. Hadjiyiannakou, K. Jansen, G. Koutsou, and A. Vaquero Aviles-Casco, *Phys. Rev. D* **102**, 054517 (2020), [arXiv:1909.00485 \[hep-lat\]](#).
- [48] S. Durr *et al.*, *Phys. Rev. Lett.* **116**, 172001 (2016), [arXiv:1510.08013 \[hep-lat\]](#).
- [49] Y.-B. Yang, A. Alexandrou, T. Draper, J. Liang, and K.-F. Liu (xQCD), *Phys. Rev. D* **94**, 054503 (2016), [arXiv:1511.09089 \[hep-lat\]](#).
- [50] G. S. Bali, S. Collins, D. Richtmann, A. Schäfer, W. Söldner, and A. Sternbeck (RQCD), *Phys. Rev. D* **93**, 094504 (2016), [arXiv:1603.00827 \[hep-lat\]](#).
- [51] M. Gong *et al.* (XQCD), *Phys. Rev. D* **88**, 014503 (2013), [arXiv:1304.1194 \[hep-ph\]](#).
- [52] A. Abdel-Rehim, C. Alexandrou, M. Constantinou, K. Hadjiyiannakou, K. Jansen, C. Kallidonis, G. Koutsou, and A. Vaquero Aviles-Casco (ETM), *Phys. Rev. Lett.* **116**, 252001 (2016), [arXiv:1601.01624 \[hep-lat\]](#).
- [53] G. S. Bali *et al.* (QCDSF), *Phys. Rev. D* **85**, 054502 (2012), [arXiv:1111.1600 \[hep-lat\]](#).
- [54] P. L. J. Petrak, G. Bali, S. Collins, J. Heitger, D. Jenkins, and S. Weishäupl, *PoS LATTICE2022*, 112 (2023), [arXiv:2301.03871 \[hep-lat\]](#).
- [55] J. Hisano, K. Ishiwata, and N. Nagata, *Phys. Rev. D* **82**, 115007 (2010), [arXiv:1007.2601 \[hep-ph\]](#).
- [56] J. Hisano, K. Ishiwata, N. Nagata, and T. Takesako, *JHEP* **07**, 005 (2011), [arXiv:1104.0228 \[hep-ph\]](#).
- [57] J. R. Ellis, K. A. Olive, and C. Savage, *Phys. Rev. D* **77**, 065026 (2008), [arXiv:0801.3656 \[hep-ph\]](#).
- [58] A. Crivellin, M. Hoferichter, and M. Procura, *Phys. Rev. D* **89**, 054021 (2014), [arXiv:1312.4951 \[hep-ph\]](#).
- [59] M. Bruno, I. Campos, P. Fritzsche, J. Koponen, C. Pena, D. Preti, A. Ramos, and A. Vladikas (ALPHA), *Eur. Phys. J. C* **80**, 169 (2020), [arXiv:1911.08025 \[hep-lat\]](#).
- [60] T. Blum *et al.* (RBC, UKQCD), *Phys. Rev. D* **93**, 074505 (2016), [arXiv:1411.7017 \[hep-lat\]](#).
- [61] S. Durr, Z. Fodor, C. Hoelbling, S. D. Katz, S. Krieg, T. Kurth, L. Lellouch, T. Lippert, K. K. Szabo, and G. Vulvert (BMW), *Phys. Lett. B* **701**, 265 (2011), [arXiv:1011.2403 \[hep-lat\]](#).
- [62] S. Durr, Z. Fodor, C. Hoelbling, S. D. Katz, S. Krieg, T. Kurth, L. Lellouch, T. Lippert, K. K. Szabo, and G. Vulvert (BMW), *JHEP* **08**, 148 (2011), [arXiv:1011.2711 \[hep-lat\]](#).
- [63] C. McNeile, C. T. H. Davies, E. Follana, K. Hornbostel, and G. P. Lepage, *Phys. Rev. D* **82**, 034512 (2010), [arXiv:1004.4285 \[hep-lat\]](#).
- [64] A. Bazavov *et al.*, *PoS LATTICE2010*, 083 (2010), [arXiv:1011.1792 \[hep-lat\]](#).
- [65] K.-F. Liu, W.-C. Chang, H.-Y. Cheng, and J.-C. Peng, *Phys. Rev. Lett.* **109**, 252002 (2012), [arXiv:1206.4339 \[hep-ph\]](#).
- [66] A. Bazavov *et al.* (MILC), *PoS CD09*, 007 (2009), [arXiv:0910.2966 \[hep-ph\]](#).
- [67] A. Bussone, A. Conigli, J. Frison, G. Herdoíza, C. Pena, D. Preti, A. Sáez, and J. Ugarrío (Alpha), *Eur. Phys. J. C* **84**, 506 (2024), [arXiv:2309.14154 \[hep-lat\]](#).
- [68] Y.-B. Yang *et al.*, *Phys. Rev. D* **92**, 034517 (2015), [arXiv:1410.3343 \[hep-lat\]](#).
- [69] K. Nakayama, B. Fahy, and S. Hashimoto, *Phys. Rev. D* **94**, 054507 (2016), [arXiv:1606.01002 \[hep-lat\]](#).
- [70] P. Petreczky and J. H. Weber, *Phys. Rev. D* **100**, 034519 (2019), [arXiv:1901.06424 \[hep-lat\]](#).
- [71] J. Heitger, F. Joswig, and S. Kuberski (ALPHA), *JHEP* **05**, 288 (2021), [arXiv:2101.02694 \[hep-lat\]](#).
- [72] R. Tarrach, *Nucl. Phys.* **B196**, 45 (1982).

- [73] T. Appelquist and J. Carazzone, *Phys. Rev. D* **11**, 2856 (1975).
- [74] R. L. Workman *et al.* (Particle Data Group), *PTEP* **2022**, 083C01 (2022).
- [75] F. He, P. Sun, and Y.-B. Yang (χ QCD), *Phys. Rev. D* **104**, 074507 (2021), arXiv:2101.04942 [hep-lat].
- [76] B. Wang, F. He, G. Wang, T. Draper, J. Liang, K.-F. Liu, and Y.-B. Yang (χ QCD), *Phys. Rev. D* **109**, 094504 (2024), arXiv:2401.05496 [hep-lat].
- [77] X.-H. Cao, F.-K. Guo, Q.-Z. Li, and D.-L. Yao, (2024), arXiv:2411.13398 [hep-ph].
- [78] D. C. Hackett, D. A. Pefkou, and P. E. Shanahan, *Phys. Rev. Lett.* **132**, 251904 (2024), arXiv:2310.08484 [hep-lat].
- [79] D. C. Hackett, P. R. Oare, D. A. Pefkou, and P. E. Shanahan, *Phys. Rev. D* **108**, 114504 (2023), arXiv:2307.11707 [hep-lat].
- [80] X. Ji, *Front. Phys. (Beijing)* **16**, 64601 (2021), arXiv:2102.07830 [hep-ph].
- [81] D. Kharzeev, *Proc. Int. Sch. Phys. Fermi* **130**, 105 (1996), arXiv:nucl-th/9601029.
- [82] Y. Hatta and D.-L. Yang, *Phys. Rev. D* **98**, 074003 (2018), arXiv:1808.02163 [hep-ph].
- [83] B. Duran *et al.*, *Nature* **615**, 813 (2023), arXiv:2207.05212 [nucl-ex].
- [84] X. Jiang, C. Shi, Y. Chen, M. Gong, and Y.-B. Yang, (2024), arXiv:2411.08461 [hep-lat].
- [85] R. G. Edwards and B. Joo (SciDAC, LHPC, UKQCD), *Lattice field theory. Proceedings, 22nd International Symposium, Lattice 2004, Batavia, USA, June 21-26, 2004*, *Nucl. Phys. Proc. Suppl.* **140**, 832 (2005), [832(2004)], arXiv:hep-lat/0409003 [hep-lat].
- [86] M. A. Clark, R. Babich, K. Barros, R. C. Brower, and C. Rebbi, *Comput. Phys. Commun.* **181**, 1517 (2010), arXiv:0911.3191 [hep-lat].
- [87] R. Babich, M. A. Clark, B. Joo, G. Shi, R. C. Brower, and S. Gottlieb, in *SC11 International Conference for High Performance Computing, Networking, Storage and Analysis Seattle, Washington, November 12-18, 2011* (2011) arXiv:1109.2935 [hep-lat].
- [88] M. A. Clark, B. Jo, A. Strelchenko, M. Cheng, A. Gambhir, and R. Brower, (2016), arXiv:1612.07873 [hep-lat].
- [89] Y.-J. Bi, Y. Xiao, M. Gong, W.-Y. Guo, P. Sun, S. Xu, and Y.-B. Yang, *Proceedings, 37th International Symposium on Lattice Field Theory (Lattice 2019): Wuhan, China, June 16-22 2019*, *PoS LATTICE2019*, 286 (2020), arXiv:2001.05706 [hep-lat].
- [90] H. Xing, J. Liang, L. Liu, P. Sun, and Y.-B. Yang, (2022), arXiv:2210.08555 [hep-lat].
- [91] H. Liu, J. He, L. Liu, P. Sun, W. Wang, Y.-B. Yang, and Q.-A. Zhang, *Sci. China Phys. Mech. Astron.* **67**, 211011 (2024), arXiv:2207.00183 [hep-lat].
- [92] H. Liu, L. Liu, P. Sun, W. Sun, J.-X. Tan, W. Wang, Y.-B. Yang, and Q.-A. Zhang, *Phys. Lett. B* **841**, 137941 (2023), arXiv:2303.17865 [hep-lat].
- [93] H. Liu, W. Wang, and Q.-A. Zhang, *Phys. Rev. D* **109**, 036037 (2024), arXiv:2309.05432 [hep-ph].
- [94] H. Yan, C. Liu, L. Liu, Y. Meng, and H. Xing, (2024), arXiv:2404.13479 [hep-lat].
- [95] Q.-A. Zhang *et al.*, *Chin. Phys. C* **46**, 011002 (2022), arXiv:2103.07064 [hep-lat].
- [96] X.-Y. Han, J. Hua, X. Ji, C.-D. Lü, W. Wang, J. Xu, Q.-A. Zhang, and S. Zhao, (2024), arXiv:2403.17492 [hep-ph].
- [97] Y. Meng, J.-L. Dang, C. Liu, Z. Liu, T. Shen, H. Yan, and K.-L. Zhang, *Phys. Rev. D* **109**, 074511 (2024), arXiv:2401.13475 [hep-lat].
- [98] Y. Meng, J.-L. Dang, C. Liu, X.-Y. Tuo, H. Yan, Y.-B. Yang, and K.-L. Zhang, *Phys. Rev. D* **110**, 074510 (2024), arXiv:2407.13568 [hep-lat].
- [99] S. Borsanyi *et al.*, *Nature* **593**, 51 (2021), arXiv:2002.12347 [hep-lat].
- [100] M. Di Carlo, D. Giusti, V. Lubicz, G. Martinelli, C. T. Sachrajda, F. Sanfilippo, S. Simula, and N. Tantalo, *Phys. Rev. D* **100**, 034514 (2019), arXiv:1904.08731 [hep-lat].

TABLE I. Lattice size $\tilde{L}^3 \times \tilde{T}$, gauge coupling $\hat{\beta}$, bare quark mass parameters $\tilde{m}_{l,s}^b$, the corresponding pseudoscalar mass m_{π,η_s} , and the statistics information.

Symbol	$\tilde{L}^3 \times \tilde{T}$	$\hat{\beta}$	a (fm)	\tilde{m}_l^b	\tilde{m}_s^b	m_π (MeV)	m_{η_s} (MeV)	$m_\pi L$	n_{cfg}	n_{src}^l	$n_{\text{src}}^{s,c}$
C24P34	$24^3 \times 64$	6.20	0.10521(11)(62)	-0.2770	-0.2310	340.2(1.7)	748.61(75)	4.38	199	32	32
C24P29	$24^3 \times 72$			-0.2770	-0.2400	292.3(1.0)	657.83(64)	3.75	760	3	3
C32P29	$32^3 \times 64$			-0.2770	-0.2400	293.1(0.8)	658.80(43)	5.01	489	3	3
C32P23	$32^3 \times 64$			-0.2790	-0.2400	227.9(1.2)	643.93(45)	3.91	400	3	3
C48P23	$48^3 \times 96$			-0.2790	-0.2400	224.1(1.2)	644.08(62)	5.79	60	3	3
C48P14	$48^3 \times 96$			-0.2825	-0.2310	136.4(1.7)	706.55(39)	3.56	136	48	3
E28P35	$28^3 \times 64$	6.308	0.08970(26)(53)	-0.2490	-0.2170	351.4(1.4)	717.94(93)	4.43	142	4	4
F32P30	$32^3 \times 96$	6.41	0.07751(14)(45)	-0.2295	-0.2050	300.4(1.2)	675.98(97)	3.81	250	3	3
F48P30	$48^3 \times 96$			-0.2295	-0.2050	302.7(0.9)	674.76(58)	5.72	99	3	3
F32P21	$32^3 \times 64$			-0.2320	-0.2050	210.3(2.3)	658.79(94)	2.67	194	3	3
F48P21	$48^3 \times 96$			-0.2320	-0.2050	207.5(1.1)	661.94(64)	3.91	75	3	3
F64P12	$64^3 \times 128$			-0.2336	-0.2030	122.8(0.9)	679.90(30)	3.09	109	4	4
G36P29	$36^3 \times 108$	6.498	0.06884(18)(41)	-0.2150	-0.1926	297.2(0.9)	693.05(46)	3.68	270	4	4
H48P32	$48^3 \times 144$	6.72	0.05198(20)(31)	-0.1850	-0.1700	316.6(1.0)	691.88(65)	4.06	157	12	12

SUPPLEMENTAL MATERIALS

1. Details of the ensembles

The ensembles used in this work are summarized in Table I. They were generated using a tadpole-improved tree-level Symanzik (TITLS) gauge action with a 2+1 flavor tadpole-improved tree-level Clover (TITLC) fermion action.

The TITLS gauge action, denoted as S_g , is defined as

$$S_g = \frac{1}{N_c} \text{Re} \sum_{x,\mu < \nu} \text{Tr} \left[1 - \hat{\beta} \left(\mathcal{P}_{\mu,\nu}^U(x) + \frac{c_1 \mathcal{R}_{\mu,\nu}^U(x)}{1 - 8c_1^0} \right) \right],$$

where $N_c = 3$,

$$\mathcal{P}_{\mu,\nu}^U(x) = U_\mu(x) U_\nu(x + a\hat{\mu}) U_\mu^\dagger(x + a\hat{\nu}) U_\nu^\dagger(x)$$

and

$$\mathcal{R}_{\mu,\nu}^U(x) = U_\mu(x) U_\mu(x + a\hat{\mu}) U_\nu(x + 2a\hat{\mu}) U_\mu^\dagger(x + a\hat{\mu} + a\hat{\nu}) U_\mu^\dagger(x + a\hat{\nu}) U_\nu^\dagger(x),$$

with the link variable $U_\mu(x)$ given by

$$U_\mu(x) = P \left[\exp \left(ig_0 \int_{x+a\hat{\mu}}^x dy B_\mu(y) \right) \right],$$

and $\hat{\beta} = (1 - 8c_1^0) \frac{6}{g_0^2 u_0^4} \equiv \frac{10}{g_0^2 u_0^4}$, with $c_1^0 = -\frac{1}{12}$, $c_1 = \frac{c_1^0}{u_0^2}$, and

$$u_0 = \left\langle \frac{\text{ReTr} \sum_{x,\mu < \nu} \mathcal{P}_{\mu,\nu}^U(x)}{6N_c \tilde{V}} \right\rangle^{1/4}$$

being the tadpole improvement factor. Here, $\tilde{V} = \tilde{L}^3 \times \tilde{T}$ is the dimensionless 4-D volume of the lattice, and we use \tilde{O} for the dimensionless value of any quantity O .

The TITLC fermion action employs a 1-step stout smeared link V with smearing parameter $\rho = 0.125$, and is given by

$$S_q(m) = \sum_{x,\mu=1,\dots,4,\eta=\pm} \bar{\psi}(x + \eta\hat{\mu}a) \frac{1 - \eta\gamma_\mu}{2} V_{\eta\mu}(x) \psi(x) + \sum_x \bar{\psi}(x) \left[-(4 + ma) \delta_{y,x} + c_{\text{sw}} \sigma^{\mu\nu} g_0 F_{\mu\nu}^V \right] \psi(x),$$

Baryon	Quark Content	Interpolating Field	I	I_z	J
p	uud	$\epsilon_{abc}P^+(d_a^T C \gamma^5 u_b)u_c$	$\frac{1}{2}$	$+\frac{1}{2}$	
Λ	uds	$\epsilon_{abc}P^+[2(u_a^T C \gamma^5 d_b)s_c + (u_a^T C \gamma^5 s_b)d_c - (d_a^T C \gamma^5 s_b)u_c]$	0	0	
Σ^+	uus	$\epsilon_{abc}P^+(s_a^T C \gamma^5 u_b)u_c$	1	+1	
Ξ^0	uss	$\epsilon_{abc}P^+(u_a^T C \gamma^5 s_b)s_c$	$\frac{1}{2}$	$+\frac{1}{2}$	
Λ_c	udc	$\epsilon_{abc}P^+[2(u_a^T C \gamma^5 d_b)c_c + (u_a^T C \gamma^5 c_b)d_c - (d_a^T C \gamma^5 c_b)u_c]$	0	0	
Σ_c^{++}	uuc	$\epsilon_{abc}P^+(c_a^T C \gamma^5 u_b)u_c$	1	+1	$\frac{1}{2}$
Ξ_c^+	usc	$\epsilon_{abc}P^+[2(u_a^T C \gamma^5 s_b)c_c + (u_a^T C \gamma^5 c_b)s_c - (s_a^T C \gamma^5 c_b)u_c]$	$\frac{1}{2}$	$+\frac{1}{2}$	
$\Xi_c'^+$	usc	$\epsilon_{abc}P^+[(u_a^T C \gamma^5 c_b)s_c + (s_a^T C \gamma^5 c_b)u_c]$	$\frac{1}{2}$	$+\frac{1}{2}$	
Ω_c^0	ssc	$\epsilon_{abc}P^+(c_a^T C \gamma^5 s_b)s_c$	0	0	
Ξ_{cc}^{++}	ucc	$\epsilon_{abc}P^+(u_a^T C \gamma^5 c_b)c_c$	$\frac{1}{2}$	$+\frac{1}{2}$	
Ω_{cc}^+	scc	$\epsilon_{abc}P^+(s_a^T C \gamma^5 c_b)c_c$	0	0	
Δ^{++}	uuu	$\epsilon_{abc}P^+(u_a^T C \gamma^\mu u_b)u_c$	$\frac{3}{2}$	$+\frac{3}{2}$	
Σ^{*+}	uus	$\epsilon_{abc}P^+[(u_a^T C \gamma^\mu u_b)s_c + 2(s_a^T C \gamma^\mu u_b)u_c]$	1	+1	
Ξ^{*0}	uss	$\epsilon_{abc}P^+[2(s_a^T C \gamma^\mu u_b)s_c + (s_a^T C \gamma^\mu s_b)u_c]$	$\frac{1}{2}$	$+\frac{1}{2}$	
Ω^-	sss	$\epsilon_{abc}P^+(s_a^T C \gamma^\mu s_b)s_c$	0	0	
Ξ^{*+}	usc	$\epsilon_{abc}P^+[(u_a^T C \gamma^\mu s_b)c_c + (s_a^T C \gamma^\mu c_b)u_c + (c_a^T C \gamma^\mu u_b)s_c]$	$\frac{1}{2}$	$+\frac{1}{2}$	$\frac{3}{2}$
Ω_c^{*0}	ssc	$\epsilon_{abc}P^+[2(s_a^T C \gamma^\mu c_b)s_c + (s_a^T C \gamma^\mu s_b)c_c]$	0	0	
Σ_c^{*++}	uuc	$\epsilon_{abc}P^+[(u_a^T C \gamma^\mu u_b)c_c + 2(c_a^T C \gamma^\mu u_b)u_c]$	1	+1	
Ξ_{cc}^{*++}	ucc	$\epsilon_{abc}P^+[2(c_a^T C \gamma^\mu u_b)c_c + (c_a^T C \gamma^\mu c_b)u_c]$	$\frac{1}{2}$	$+\frac{1}{2}$	
Ω_{cc}^{*+}	scc	$\epsilon_{abc}P^+[2(c_a^T C \gamma^\mu s_b)c_c + (c_a^T C \gamma^\mu c_b)s_c]$	0	0	
Ω_{ccc}^{++}	ccc	$\epsilon_{abc}P^+(c_a^T C \gamma^\mu c_b)c_c$	0	0	

TABLE II. Interpolating fields for baryons.

where $c_{\text{sw}} = \frac{1}{v_0^3}$ with $v_0 = \left\langle \frac{\text{ReTr} \sum_{x,\mu < \nu} \mathcal{P}_{\mu\nu}^V(x)}{6N_c V} \right\rangle^{1/4}$, and

$$F_{\mu\nu}^V = \frac{i}{8a^2 g_0} (\mathcal{P}_{\mu,\nu}^V - \mathcal{P}_{\nu,\mu}^V + \mathcal{P}_{\nu,-\mu}^V - \mathcal{P}_{-\mu,\nu}^V + \mathcal{P}_{-\mu,-\nu}^V - \mathcal{P}_{-\nu,-\mu}^V + \mathcal{P}_{-\nu,\mu}^V - \mathcal{P}_{\mu,-\nu}^V).$$

Based on the joint fit on subsets of these ensembles with several lattice spacing, quark masses and volumes [2, 3], the physical up, down, strange and charm quark masses and also related CKM matrix elements $V_{u(c)d(s)}$ agree with the current lattice averages well [28]. These ensembles have been also used to study the hadron spectrum [90–94] and structures [95–98].

2. Interpolation fields, 2-point functions and ground state baryon mass extraction

For the interpolation fields of the baryons, we use $\epsilon_{abc}P^+ [(q_a^1)^T C \gamma^5 q_b^2] q_c^3$ and $\epsilon_{abc}P^+ [(q_a^1)^T C \gamma^\mu q_b^2] q_c^3$ for the spin-1/2 and 3/2 particles, respectively. Note that some of the particles require linear combination of different permutations of three quarks. The interpolation fields for the baryons we investigated in this work are summarized in Table II. For baryons with light (up and/or down) quarks, we maximize the number of up quarks in the interpolation field, as the other configurations are equivalent due to isospin symmetry.

As presented in Table I, we computed the Coulomb gauge fixed source propagators at n_{src}^l time slices for each configuration at three light quark masses including the unitary one, and at $n_{\text{src}}^{s,c}$ for three strange and charm quark masses. We have 23,845 (for the proton and Δ baryon) and 17,725 (for the other baryons) measurements on the 3,340 configurations of 14 ensembles in total.

Taking the nucleon as example, the the wall-to-point two-point functions we used in the this work is, explicitly

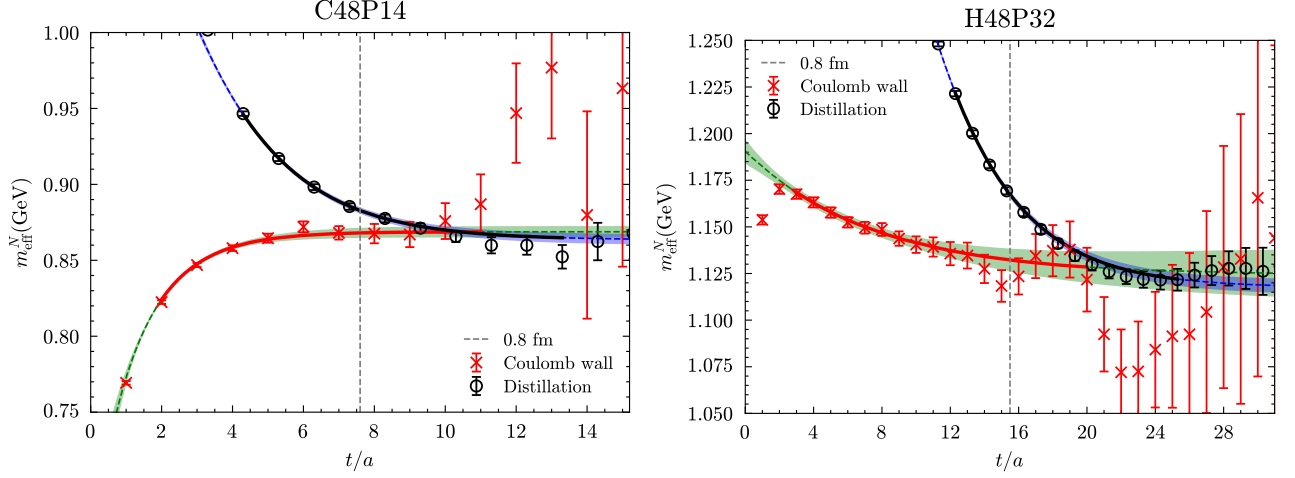


FIG. 3. The effective mass obtained from the two-point correlation functions (2pt) of the nucleon in two representative ensembles: the physical point ensemble C48P14 (left panel) and the ensemble with the finest lattice spacing, H48P32 (right panel). The effective mass derived from the 2pt correlation functions (using a Coulomb wall source and point sink, indicated by red crosses) is compared with the results obtained using the distillation method (shown as black circles). Both methods exhibit good agreement in the plateau region, despite different initial trends with respect to t/a . The green bands represent the ground state mass that we extracted.

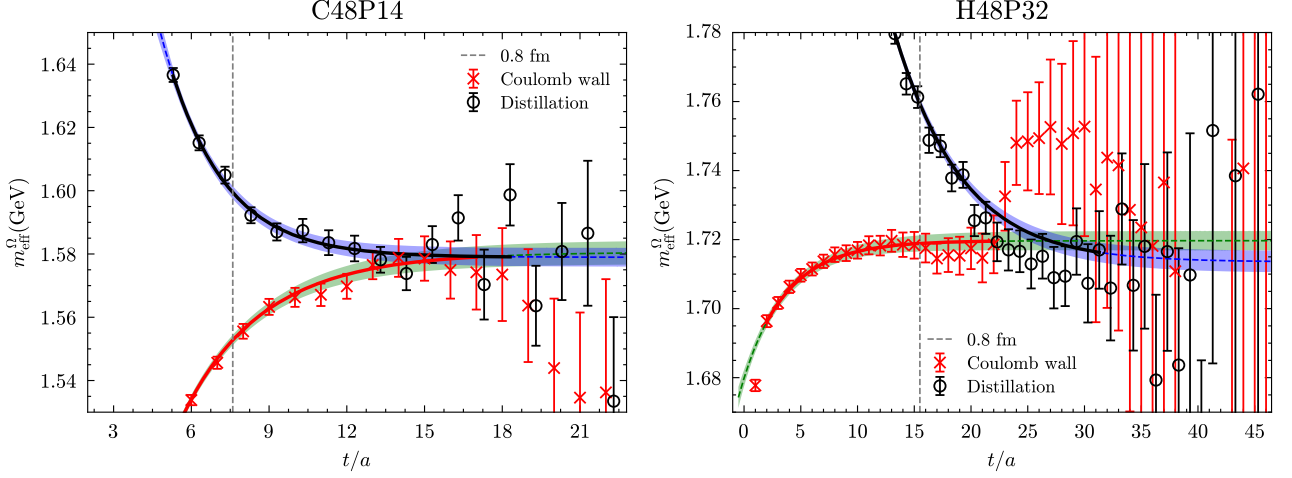
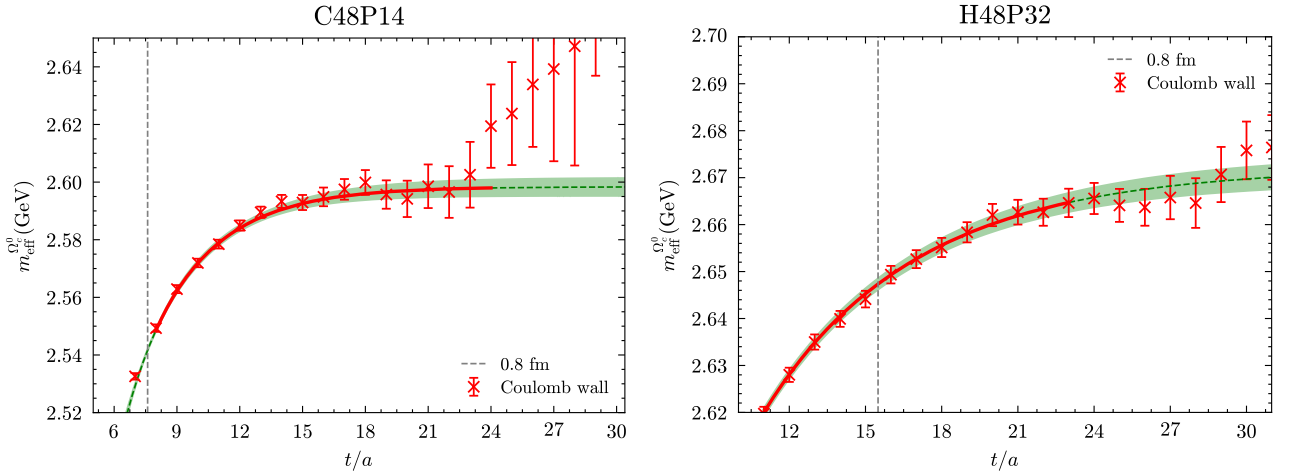
recovering the coordinate and Dirac indices,

$$C_{2,N}^{wp}(y^0, x^0) = \sum_{\vec{x}, \vec{y}} \langle \chi_N^\alpha(y) \bar{\chi}_N^\alpha(x) \rangle = \sum_{\vec{y}} \epsilon_{abc} \epsilon_{a'b'c'} \left\langle (C\gamma_5)^{\alpha'\beta'} (C\gamma_5)^{\alpha\beta} (P^\pm)^{\gamma\gamma'} S_d^C(y, x^0)_{\alpha'\alpha} \right. \\ \left. \times \left[S_u^C(y, x^0)_{\beta'\beta} S_u^C(y, x^0)_{\gamma'\gamma} - S_u^C(y, x^0)_{\beta'\gamma} S_u^C(y, x^0)_{\gamma'\beta} \right] \right\rangle, \quad (4)$$

where the Coulomb gauge-fixed wall propagator is defined by $S_q^C(y, x^0) \equiv \sum_{\vec{x}} S(y, x; U_C; \tilde{m}_q^b)$ as used in Ref. [2], and $S(y, x; U_C) = \psi(y; U_C) \bar{\psi}(x; U_C)$ is the standard quark propagator computed with the gauge configuration U . The Coulomb gauge-fixed configuration U_C satisfies the discretized gauge-fixing condition $\text{Im} \left[\sum_{i=1}^3 (U_C(x) - U_C(x - a\hat{n}_i)) \right] = 0$.

In Fig. 3-5, we present the effective logarithmic mass obtained from two-point correlators for three baryons—the nucleon, Ω , and Ω_c —on two representative ensembles: the physical point ensemble C48P14 and the finest lattice spacing ensemble H48P32. The results are shown using the Coulomb wall source (red crosses) and, where available, the distillation method (black circles) from CLQCD collaborators.

For both the nucleon and Ω baryons, we observe that the effective masses from the Coulomb wall source and distillation method are in good agreement once the plateau is reached, even though the initial trends with respect to t/a differ; specifically, the Coulomb wall source tends to increase with t , while the distillation results exhibit a decrease before stabilizing. This consistency at the plateau confirms the reliability of both approaches. Even though no comparative distillation data is available for the Ω_c baryon, the statistical uncertainty here is small enough to ensure the reliability of the fit. The green (blue) bands in each plot indicate the fit uncertainties for the extracted effective masses which consistent with the original data points well.

FIG. 4. Similar figures for the Ω baryon.FIG. 5. Similar figures for the Ω_c baryon, while the distillation case is not available.

3. Joint fit of the baryon mass

We fit the nucleon mass using the the SU(4|2) partially quenched heavy baryon chiral perturbative theory (χ PT) ansatz [8, 27],

$$\begin{aligned}
 m_H(m_\pi^{\text{val}}, m_\pi^{\text{sea}}, m_{\eta_s}^{\text{sea}}, a, 1/L) = & m_H^{\text{phys}} + \sum_{\text{tag=val/pq}, j=2,3} C_j^{\text{tag}} [(m_\pi^{\text{tag}})^j - (m_\pi^{\text{phys}})^j] + C_s [(m_{\eta_s}^{\text{sea}})^2 - (m_{\eta_s}^{\text{phys}})^2] \\
 & + C_L \frac{(m_\pi^{\text{val}})^2}{L} e^{-m_\pi^{\text{val}} L} + \sum_i C_a^{2i} a^{2i}, \quad (5)
 \end{aligned}$$

where m_π^{val} and m_π^{sea} are the valence and sea pion masses respectively, $m^{\text{pq}} = \sqrt{(m_\pi^{\text{val}})^2 + (m_\pi^{\text{sea}})^2}$ is the partially quenched pion mass, $m_\pi^{\text{phys}} = 134.98$ MeV is the physical π^0 mass, and $m_{\eta_s}^{\text{phys}} = 689.89(49)$ MeV from Ref. [99] is the pure QCD η_s mass which corresponds to the physical strange quark mass.

In Fig. 6, we present the nucleon mass at five different lattice spacings as colored data points, with the mismatch effects between m_π^{val} and m_π^{sea} are corrected using the joint fit which gives $\chi^2/\text{d.o.f.} = 1.2$. Redefinition of parameters $C_3^{\text{val}} = \frac{(g_A^2 - 4g_A g_1 - 5g_1^2)\pi}{3(4\pi f_\pi)^2}$ and $C_3^{\text{pq}} = \frac{(8g_A^2 + 4g_A g_1 + 5g_1^2)\pi}{3(4\pi f_\pi)^2}$ are used to be consistent with the previous studies [8, 27]. The

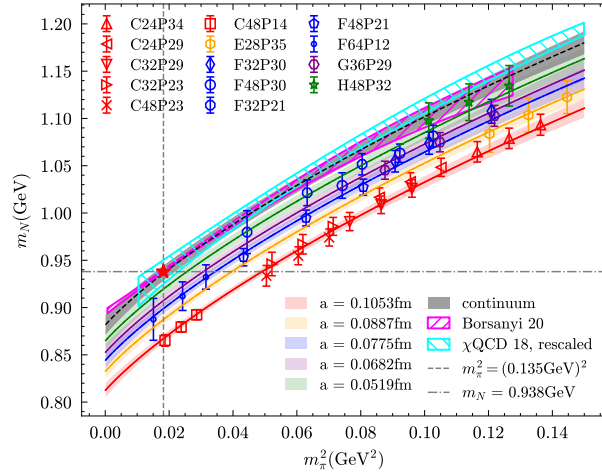


FIG. 6. The nucleon mass on 14 ensembles at 5 lattice spacings (colored data points and bands), and also that in the continuum (gray band). The mismatch effect from the unequal valence and sea pion masses has been corrected based on the joint fit. The continuum extrapolated results using the overlap fermion [8] (rescaled to match the physical nucleon mass) and staggered fermion [30] are also illustrated for comparison.

colored bands corresponds to the fit prediction at respective lattice spacings, and they agree with the data points well. Based on the linear a^2 extrapolation, our continuum extrapolated result as function of pion mass is shown as gray band, which perfectly agree with the that from using the overlap fermion [8] and staggered fermion [30]. The physical nucleon mass is shown as the red star. Note that the band from Ref. [8] is rescaled by a factor 0.978(16) from the original data to match the physical point.

For the light baryons containing a strange quark, we calculate the baryon masses using three different valance strange quark masses for each ensemble. We then interpolate the valance strange quark mass to the value corresponding to the artificial η_s (unmixed $\bar{s}s$) mass $m_{\eta_s}^{\text{phys}} = 689.89(49)$ MeV [99], which is determined by using the physical strange quark mass and is consistent with the value of 687.4(2.2) MeV [2] obtained from CLQCD ensembles, albeit with a larger uncertainty. We will revisit this strategy in the next section. The m_π^3 terms are omitted because χ PT is not applicable here, and their coefficients show no significant signal in any baryon containing strange or charm valance quarks.

The cases of charmed baryons are also similar. Following the the GRS renormalization scheme $m_{q,\text{QCD}+\text{QED}}^{\overline{\text{MS}}}(2\text{GeV}) = m_{q,\text{QCD}}^{\overline{\text{MS}}}(2\text{GeV})$, we use the pure QCD value $m_{D_s} = 1966.7(1.5)$ MeV [100] to determine the interpolated valance charm quark mass for each ensemble. The resulting masses of open and closed charmed mesons, as well as their decay constants, agree well with experimental values and lattice averages [3].

The interpolation of valance strange and charm quark masses significantly suppresses the discretization errors from the heavy quark, and also allows us to use a similar ansatz as that used for nucleons to fit the baryon mass for different flavors and angular momentum. For the charmed baryon, we retain the a^4 term in the extrapolation, as the linear a^2 extrapolation does not describe the data well, resulting in poor χ^2 . We also take $m_\pi^{\text{val}} = m_\pi^{\text{sea}}$ and drop the $(m_\pi^{\text{tag}})^{2,3}$ terms for baryon without valance light quark.

In Fig. 7, we show the lattice spacing dependence of the nucleon, Ω and Ω_c masses, with the light and strange quark masses corrected to their physical value based on the joint fit on 14 ensembles. The gray bands indicate the fit uncertainties, and the red stars correspond to the experimental values. Obviously the linear a^2 dependence describe the data of nucleon and Ω well, while the a^4 term is essential fo the Ω_c . For a comprehensive view, we present the results for all baryons in Fig. 8, whrere we apply an a^2 extrapolation for light baryons, while for charmed baryons, an a^4 extrapolation is used to capture higher-order discretization effects.

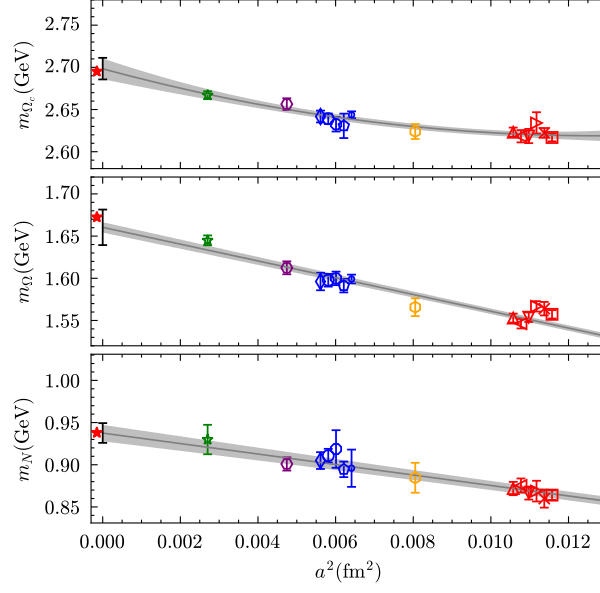


FIG. 7. Fitting results for nucleon, Ω , and Ω_c masses as functions of a^2 . The other non-physical effects for the data points are fixed using the global fit. For lattice spacings with more than one ensemble, data points are horizontally displaced for clarity.

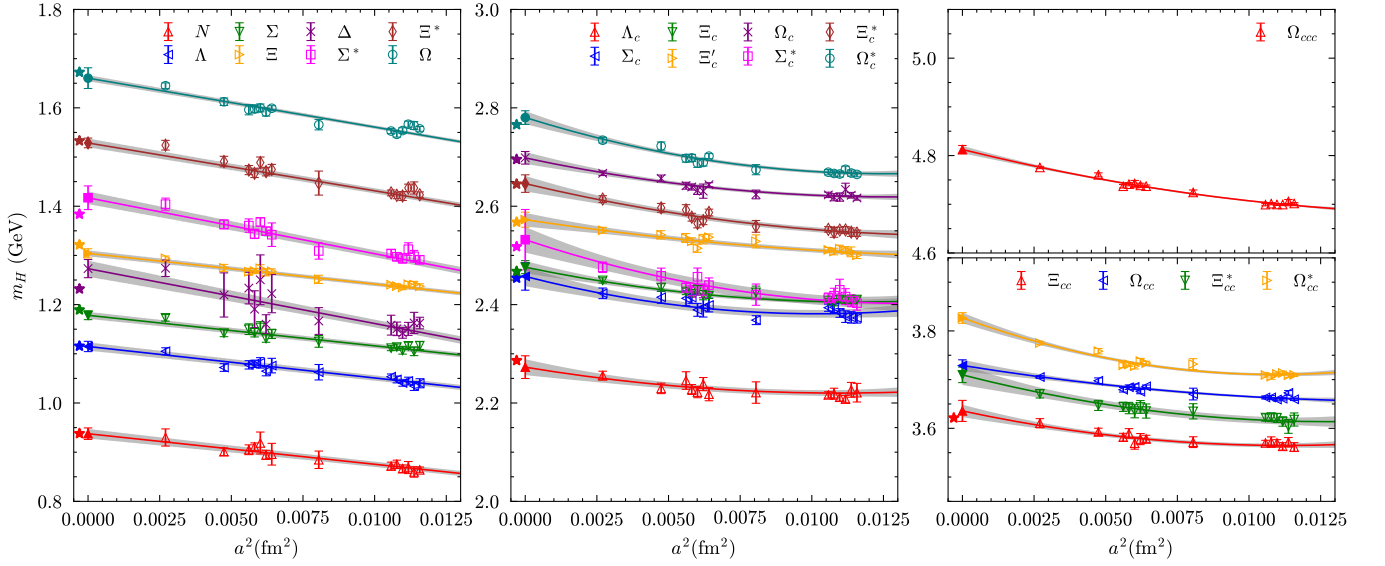


FIG. 8. Fitting results for the masses of all baryons, showing their dependence on lattice spacing a^2 . For light baryons, an a^2 extrapolation is applied, while for charmed baryons, an a^4 extrapolation is used where necessary. The gray bands represent fit uncertainties, and colored stars indicate experimental values when available. All data points have been corrected for non-physical effects using the global fit, demonstrating consistent treatment of discretization effects across the baryon spectrum. For lattice spacings with more than one ensemble, data points are horizontally displaced for clarity.

4. σ_{qH} extraction

The Feynman-Hellman theorem establishes the relation $\langle \bar{q}q \rangle_H = \frac{\partial m_H}{\partial m_q}$, which can be further decomposed into contributions from valence and sea quarks:

$$\langle \bar{q}q \rangle_H = \langle \bar{q}q \rangle_H^{\text{val}} + \langle \bar{q}q \rangle_H^{\text{sea}}, \quad \langle \bar{q}q \rangle_H^{\text{val}} = \frac{\partial m_H(m_q^{\text{val}}, m_q^{\text{sea}})}{\partial m_q^{\text{val}}}, \quad \langle \bar{q}q \rangle_H^{\text{sea}} = \frac{\partial m_H(m_q^{\text{val}}, m_q^{\text{sea}})}{\partial m_q^{\text{sea}}}. \quad (6)$$

Here, $m_q^{\text{val/sea}}$ denote the valence/sea quark masses, and $m_H(m_q^{\text{val}}, m_q^{\text{sea}})$ is derived from joint fits of lattice data across ensembles with varying m_q^{val} and m_q^{sea} . The valence term $\langle \bar{q}q \rangle_H^{\text{val}}$ can first be extracted on individual ensembles and then extrapolated to the physical quark masses, infinite volume, and continuum limit through a global fit.

Since the valence strange and charm quark masses ($m_{s,c}^{\text{val}}$) are tuned to reproduce the pure-QCD masses m_{η_s} and m_{D_s} on each ensemble (where sea quark masses $m_{l,s}^{\text{sea}}$ may deviate from physical values), mismatches $\delta m_{l,s}^s \equiv m_{l,s}^{\text{sea}} - m_{l,s}^{\text{phys}}$ induce corrections to the valence masses: $\delta \mathbf{m}_{s,c}^{\text{val}} \equiv m_{s,c}^{\text{val}} - m_{s,c}^{\text{phys}}$ with the following constraints:

$$\begin{aligned} 0 &= \delta m_{\eta_s} = \delta m_l^s \langle \bar{l}l \rangle_{\eta_s}^{\text{sea}} + \delta \mathbf{m}_s^{\text{val}} \langle \bar{s}s \rangle_{\eta_s}^{\text{val}} + \delta m_s^{\text{sea}} \langle \bar{s}s \rangle_{\eta_s}^{\text{sea}}, \\ 0 &= \delta m_{D_s} = \delta m_l^s \langle \bar{l}l \rangle_{D_s}^{\text{sea}} + \delta \mathbf{m}_s^{\text{val}} \langle \bar{s}s \rangle_{D_s}^{\text{val}} + \delta m_s^{\text{sea}} \langle \bar{s}s \rangle_{D_s}^{\text{sea}} + \delta \mathbf{m}_c^{\text{val}} \langle \bar{c}c \rangle_{D_s}^{\text{val}}, \end{aligned} \quad (7)$$

where all the condensates correspond to those at physical quark masses. The resulting correction to any hadron mass m_H is:

$$\begin{aligned} \delta m_H &= \delta m_l^{\text{sea}} \langle \bar{l}l \rangle_H^{\text{sea}} + \delta \mathbf{m}_s^{\text{val}} \langle \bar{s}s \rangle_H^{\text{val}} + \delta m_s^{\text{sea}} \langle \bar{s}s \rangle_H^{\text{sea}} + \delta \mathbf{m}_c^{\text{val}} \langle \bar{c}c \rangle_H^{\text{val}} \\ &= \delta m_l^{\text{sea}} \left(\langle \bar{l}l \rangle_H^{\text{sea}} + \frac{\partial \mathbf{m}_s^{\text{val}}}{\partial m_l^{\text{sea}}} \langle \bar{s}s \rangle_H^{\text{val}} + \frac{\partial \mathbf{m}_c^{\text{val}}}{\partial m_l^{\text{sea}}} \langle \bar{c}c \rangle_H^{\text{val}} \right) + \delta m_s^{\text{sea}} \left(\langle \bar{s}s \rangle_H^{\text{sea}} + \frac{\partial \mathbf{m}_s^{\text{val}}}{\partial m_s^{\text{sea}}} \langle \bar{s}s \rangle_H^{\text{val}} + \frac{\partial \mathbf{m}_c^{\text{val}}}{\partial m_s^{\text{sea}}} \langle \bar{c}c \rangle_H^{\text{val}} \right). \end{aligned} \quad (8)$$

Thus, when extracting $\langle \bar{l}l \rangle_H^{\text{sea}}$ from the light quark mass dependence of m_H , contamination from $\delta \mathbf{m}_{s,c}^{\text{val}}$ must be subtracted.

After this subtraction, the sigma terms used in this work are defined as:

$$\begin{aligned} \sigma_{\pi H} &= \sigma_{\pi H}^{\text{val}} + \sigma_{\pi H}^{\text{sea}}, \\ \sigma_{\pi H}^{\text{val,H}} &\equiv (m_{\pi}^{\text{phys}})^2 \left. \frac{\partial m_H(m_{\pi}^{\text{val}}, m_{\pi}^{\text{phys}}, m_{\eta_s}^{\text{phys}}, 0, 0)}{\partial (m_{\pi}^{\text{val}})^2} \right|_{m_{\pi}^{\text{val}}=m_{\pi}^{\text{phys}}}, \end{aligned} \quad (9)$$

$$\sigma_{\pi H}^{\text{sea}} \equiv (m_{\pi}^{\text{phys}})^2 \left[\left. \frac{\partial m_H(m_{\pi}^{\text{phys}}, m_{\pi}^{\text{sea}}, m_{\eta_s}^{\text{phys}}, 0, 0)}{\partial (m_{\pi}^{\text{sea}})^2} \right|_{m_{\pi}^{\text{sea}}} - d_l^s \frac{\sigma_{s,H}^{\text{val}}}{m_s^{\text{phys}}} - d_l^c \frac{\sigma_{c,H}^{\text{val}}}{m_c^{\text{phys}}} \right], \quad (10)$$

$$\begin{aligned} \sigma_{sH} &= \sigma_{sH}^{\text{val}} + \sigma_{sH}^{\text{sea}}, \\ \sigma_{sH}^{\text{val}} &\equiv \sigma_{sH}^{\text{val}}(m_{\pi}^{\text{sea}}, m_{\eta_s}^{\text{phys}}, 0, 0), \end{aligned} \quad (11)$$

$$\sigma_{sH}^{\text{sea}} \equiv (m_{\eta_s}^{\text{phys}})^2 \left[\left. \frac{\partial m_H(m_{\pi}^{\text{phys}}, m_{\pi}^{\text{phys}}, m_{\eta_s}^{\text{sea}}, 0, 0)}{\partial (m_{\eta_s}^{\text{sea}})^2} \right|_{m_{\eta_s}^{\text{sea}}} - d_s^s \frac{\sigma_{s,H}^{\text{val}}}{m_s^{\text{phys}}} - d_s^c \frac{\sigma_{c,H}^{\text{val}}}{m_c^{\text{phys}}} \right], \quad (12)$$

$$\sigma_{cH}^{\text{val}} \equiv \sigma_{cH}^{\text{val}}(m_{\pi}^{\text{sea}}, m_{\eta_s}^{\text{phys}}, 0, 0), \quad (13)$$

where m_H is defined in Eq. (5) with tuned valence strange and charm quark masses.

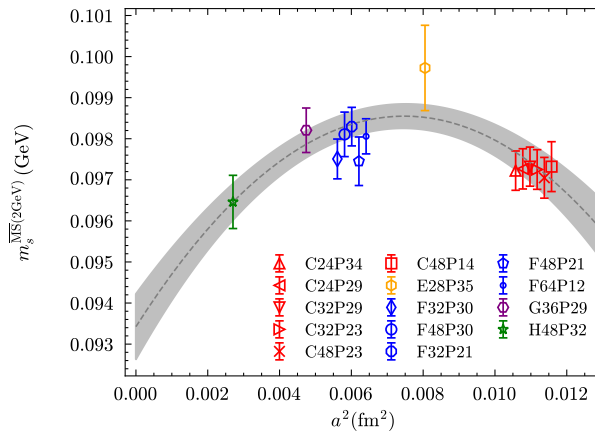


FIG. 9. Lattice spacing dependence of the renormalized strange quark mass at $\overline{\text{MS}}(2 \text{ GeV})$. The values at finite lattice spacings are corrected to the physical pion and η_s masses based on the joint fit. For lattice spacings with more than one ensemble, data points are horizontally displaced for clarity.

The coefficients $d_l^{s(c)}$ arise from joint fits of the renormalized strange and charm quark masses:

$$m_{s(c)}^{\text{val,R}} = m_{s,c}^{\text{phys,R}} + d_l^{s(c)} \left((m_\pi^{\text{sea}})^2 - (m_\pi^{\text{phys}})^2 \right) + d_s^{s(c)} \left((m_{\eta_s}^{\text{sea}})^2 - (m_{\eta_s}^{\text{phys}})^2 \right) + \sum_{i=1}^2 d_{a,i}^{s(c)} a^{2i} + d_L^{s(c)} e^{-m_\pi L}. \quad (14)$$

For the charm quark, we obtain $d_l^c = -0.161(11) (\text{GeV})^{-1}$, $d_s^c = -0.388(44) (\text{GeV})^{-1}$, and a physical renormalized mass $m_c^{\text{phys,R}} = 1.0989(89) \text{ GeV}$ in the $\overline{\text{MS}}$ scheme at 2 GeV. A similar fit for the strange quark yields $d_l^s = -0.0267(30) (\text{GeV})^{-1}$, $d_s^s = -0.0090(10) (\text{GeV})^{-1}$, and $m_s^{\text{phys,R}} = 0.09345(79) \text{ GeV}$ in the $\overline{\text{MS}}$ scheme at 2 GeV. As shown in Fig. 9, the a^4 discretization correction to $m_s^{\text{phys,R}}$ based on m_{η_s} is also significant, while the continuum extrapolated $m_s^{\text{phys,R}}$ is still consistent with our previous estimate $0.0978(21)(40) \text{ MeV}$ in Ref. [2].

The valence strange (charm) sigma term $\sigma_{s(c)H}^{\text{val}}$ defined in Eqs. (11) and (13) are extracted from the joint fit of the sigma term at each ensemble using the Feynman-Hellman theorem with the renormalized valence quark mass $m_{s(c)}^{\text{val,R}}$,

$$\begin{aligned} \sigma_{s(c)H}^{\text{val}}(m_\pi^{\text{sea}}, m_{\eta_s}^{\text{sea}}, a, 1/L) &\equiv m_{s(c)}^{\text{val,R}}(m_\pi^{\text{sea}}, m_{\eta_s}^{\text{sea}}, a, 1/L) \frac{\partial m_H(m_\pi^{\text{sea}}, m_{\eta_s}^{\text{sea}}, a, 1/L)}{\partial m_{s(c)}^{\text{val,R}}(m_\pi^{\text{sea}}, m_{\eta_s}^{\text{sea}}, a, 1/L)} \\ &= \sigma_{s(c)H}^{\text{val}}(m_\pi^{\text{phys}}, m_{\eta_s}^{\text{phys}}, 0, 0) + C_l^{\sigma_{s(c)H}} \left((m_\pi^{\text{sea}})^2 - (m_\pi^{\text{phys}})^2 \right) + C_s^{\sigma_{s(c)H}} \left((m_{\eta_s}^{\text{sea}})^2 - (m_{\eta_s}^{\text{phys}})^2 \right) \\ &\quad + \sum_i C_{a,i}^{\sigma_{s(c)H}} a^{2i} + C_L^{\sigma_{s(c)H}} e^{-m_\pi L}, \end{aligned} \quad (15)$$

Discretization errors for σ_{sH}^{val} are modeled with a^2 terms, while both a^2 and a^4 terms are needed for σ_{cH}^{val} .

In above expressions, the m_π^2 dependence approximates the light quark mass (m_l) dependence, as higher-order chiral corrections ($\sim 2\%$) [2] are negligible compared to statistical uncertainties. Similarly, $m_{\eta_s}^2/m_s \approx 4.9(1)$ [2] near the physical m_s justifies using $m_{\eta_s}^2$ to model m_s dependence.

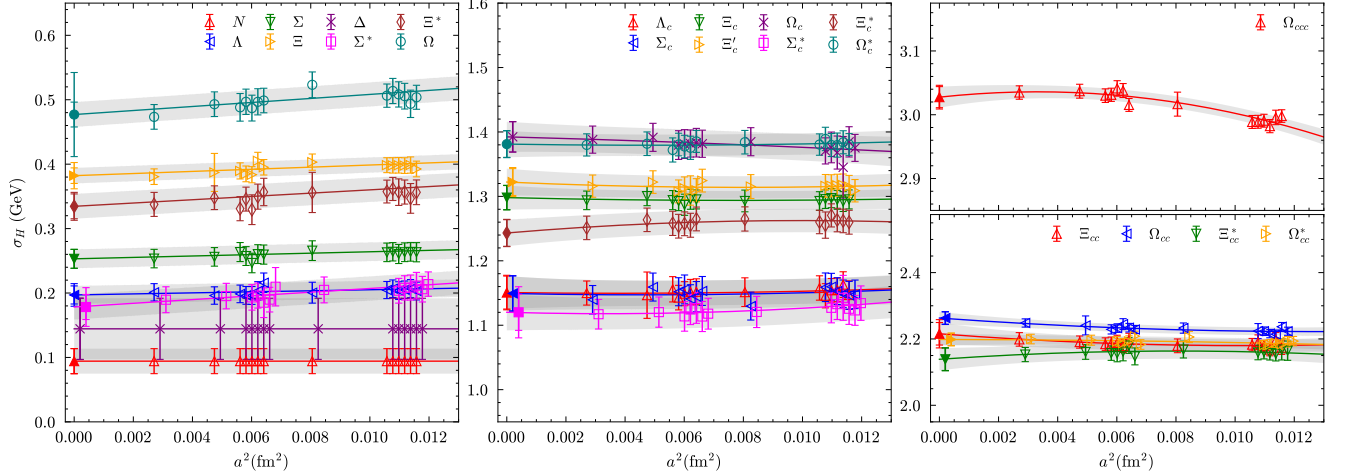


FIG. 10. Similar to Fig. 8 but for σ_H . The plots indicate that the discretization effects on σ_H are generally smaller than those observed for the baryon masses, though the associated uncertainties are comparatively larger. Data points are horizontally displaced for clarity.

In Fig. 10, we present the plots of σ_H for all baryons, similar to Fig. 8 for the baryon masses. As indicated in the figure, the discretization effects on σ_H are generally smaller than those on the total baryon mass, highlighting the stability of σ_H under different lattice spacings.

In Fig. 11, we present the ratio $R_{q,H} \equiv (1+\gamma_m)\sigma_{q,H}/(n_q m_q)$ for various quark flavors q in different hadrons H , where n_q denotes the number of valence quarks of flavor q . The results are given in the $\overline{\text{MS}}$ scheme at 2 GeV. Although $R_{q,H}$ itself depends on the renormalization scale and scheme, the **relative** ratio $R_{q,H}$ across different hadrons and quark flavors is scale- and scheme-independent. If we normalize all $R_{q,H}$ values by $R_{c\Omega_{ccc}}$, we find that $R_{sH}/R_{c\Omega_{ccc}} \approx 2$ for all baryons, while $R_{\pi H}/R_{c\Omega_{ccc}}$ is even larger.

Based on the similar procedure, we can also obtain the sigma term and trace anomaly for the charmed meson discussed in Ref. [3]. The comparison of $\sigma_{\pi H}$ for hadrons H with and without valence light quarks reveals that

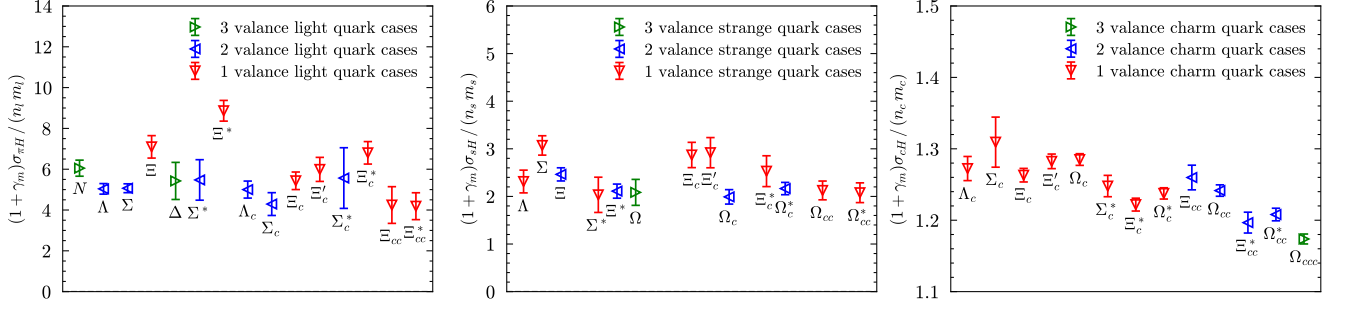


FIG. 11. Ratio $(1 + \gamma_m)\sigma_{q,H}/(n_q m_q)$ for the light (left), strange (middle) and charm (right) quark in different hadron H , at $\overline{\text{MS}}$ 2 GeV.

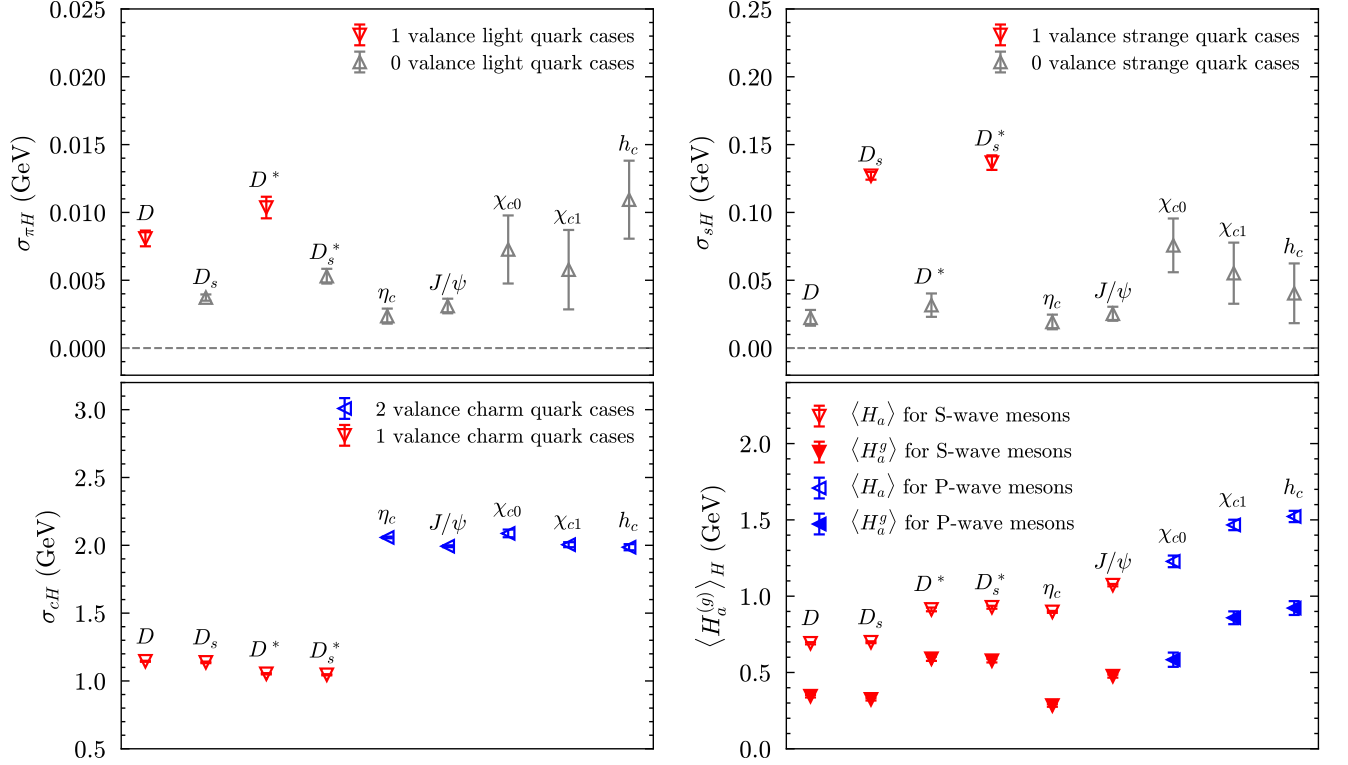


FIG. 12. Results for quark sigma terms and trace anomaly contributions to charmed meson masses. The upper-left, upper-right, and lower-left panels show the σ terms for light, strange, and charm quarks, respectively, with colors indicating the number of valence quark (and anti-quark): gray (0), red (1), blue (2). The lower-right panel presents the trace anomaly $\langle H_a \rangle_H$ and the gluon trace anomaly $\langle H_a^g \rangle_H$, with red triangles for S-wave meson and blue triangles for P-wave meson.

valence and sea contributions are comparable, as shown in Fig. 12. We also observe that the gluon trace anomaly of pseudoscalar mesons is generally smaller than that of baryons after subtracting the γ_m contribution at $\overline{\text{MS}}$ 2 GeV. Simultaneously, the trace anomalies of vector and P-wave charmed mesons appear somewhat larger, though none exceed 1 GeV like the $3/2^+$ baryon case. Further investigation of other excited charmed hadrons would be valuable for understanding the role of trace anomaly in their mass generation.

5. Error budget of our predictions

In table III, we summarized the final numerical results of the baryon masses, sigma terms and also trace anomaly contributions.

The statistical uncertainty is categorized by its sources: the statistical fluctuations in the dimensionless pion and η_s masses in the sea quark sector, the lattice spacing determination using gradient flow (excluding systematic effects from the scale parameter v taken from literature [28]), and those from the dimensionless two-point correlation functions.

For systematic uncertainties related to the scale parameter $w_0 = 0.1736(9)$ fm [28]), we perform a complete reanalysis by varying the central w_0 value by 1σ and take the resulting difference in central values as the systematic uncertainty from lattice spacing. Additional systematic uncertainties are considered from:

- 1) The experimental D_s mass measurement;
- 2) Choice of fit ansatz (additive vs. multiplicative discretization errors);
- 3) Sea quark dependence parameters $d_{1,2}^{s(c)}$ in Eqs. (10) and (12), which propagate to uncertainties of the sea quark mass contribution of sigma terms, and then also that of the gluon trace anomaly due to the sum rule.

The primary source of uncertainty is statistical, arising from the original two-point function, while scale setting can also contribute significantly to systematic uncertainty, particularly for charmed hadrons.

TABLE III: Error budget for baryon masses, sigma terms, and trace anomalies (all in GeV).

		m_H	$\sigma_{\pi H}^{\text{val}}$	$\sigma_{\pi H}^{\text{sea}}$	$\sigma_{\pi H}$	σ_{sH}^{val}	σ_{sH}^{sea}	σ_{sH}	σ_{cH}^{val}	σ_H	$\langle H_a \rangle_H$	$\langle H_a^g \rangle_H$
N	Central value	0.9376	0.0291	0.0184	0.0475	0	0.0468	0.0468	-	0.0942	0.8434	0.8156
	Statistical (total)	0.0098	0.0017	0.0019	0.0025	0	0.0176	0.0176	-	0.0194	0.0217	0.0270
	Sea π mass	0.0006	<0.0001	0.0001	<0.0001	0	0.0004	0.0004	-	0.0004	0.0007	0.0008
	Sea η_s mass	0.0025	<0.0001	<0.0001	<0.0001	0	0.0008	0.0008	-	0.0007	0.0026	0.0026
	Lattice spacing	0.0015	0.0001	<0.0001	0.0001	0	0.0007	0.0007	-	0.0009	0.0012	0.0013
	2-point function	0.0093	0.0017	0.0019	0.0025	0	0.0176	0.0176	-	0.0194	0.0215	0.0268
	Systematic (total)	0.0065	0.0009	0.0008	0.0018	0	0.0007	0.0007	-	0.0022	0.0087	0.0093
	Scale setting	0.0042	0.0002	<0.0001	0.0002	0	0.0006	0.0006	-	0.0009	0.0051	0.0054
	fit ansatz	0.0050	0.0009	0.0008	0.0018	0	0.0004	0.0004	-	0.0020	0.0070	0.0076
Sea quark correction	-	-	0	0	-	0	0	-	0	0	0	
Λ	Central value	1.1149	0.0151	0.0113	0.0264	0.1467	0.0241	0.1708	-	0.1970	0.9179	0.8598
	Statistical (total)	0.0083	0.0005	0.0011	0.0012	0.0051	0.0183	0.0176	-	0.0175	0.0193	0.0240
	Sea π mass	0.0010	<0.0001	<0.0001	<0.0001	0.0004	0.0008	0.0009	-	0.0013	0.0008	0.0013
	Sea η_s mass	0.0019	<0.0001	<0.0001	<0.0001	0.0007	0.0016	0.0015	-	0.0016	0.0010	0.0009
	Lattice spacing	0.0016	<0.0001	<0.0001	<0.0001	0.0004	0.0011	0.0010	-	0.0010	0.0019	0.0021
	2-point function	0.0079	0.0005	0.0011	0.0012	0.0050	0.0182	0.0175	-	0.0173	0.0192	0.0239
	Systematic (total)	0.0063	0.0003	0.0003	0.0006	0.0010	0.0010	0.0014	-	0.0020	0.0082	0.0087
	Scale setting	0.0039	<0.0001	<0.0001	0.0001	0.0010	<0.0001	0.0010	-	0.0011	0.0051	0.0054
	fit ansatz	0.0050	0.0003	0.0003	0.0006	<0.0001	0.0007	0.0007	-	0.0014	0.0064	0.0068
Sea quark correction	-	-	<0.0001	<0.0001	-	0.0007	0.0007	-	0.0007	0.0007	0.0009	
Σ	Central value	1.1783	0.0120	0.0146	0.0265	0.1849	0.0418	0.2267	-	0.2531	0.9252	0.8505
	Statistical (total)	0.0071	0.0003	0.0011	0.0011	0.0034	0.0153	0.0149	-	0.0146	0.0163	0.0202
	Sea π mass	0.0007	<0.0001	<0.0001	<0.0001	0.0005	0.0019	0.0018	-	0.0019	0.0021	0.0026
	Sea η_s mass	0.0021	<0.0001	<0.0001	<0.0001	0.0006	0.0008	0.0005	-	0.0005	0.0021	0.0020
	Lattice spacing	0.0008	<0.0001	<0.0001	<0.0001	0.0002	0.0010	0.0010	-	0.0010	0.0012	0.0014
	2-point function	0.0067	0.0003	0.0011	0.0011	0.0033	0.0151	0.0148	-	0.0144	0.0160	0.0199
	Systematic (total)	0.0052	0.0000	0.0001	0.0001	0.0011	0.0013	0.0019	-	0.0020	0.0068	0.0073
	Scale setting	0.0052	<0.0001	<0.0001	<0.0001	0.0011	0.0003	0.0014	-	0.0015	0.0067	0.0072
	fit ansatz	0.0004	<0.0001	<0.0001	<0.0001	<0.0001	0.0009	0.0008	-	0.0009	0.0006	0.0008
Sea quark correction	-	-	<0.0001	<0.0001	-	0.0009	0.0009	-	0.0009	0.0009	0.0012	
Ξ	Central value	1.3042	0.0074	0.0112	0.0186	0.3075	0.0562	0.3636	-	0.3822	0.9220	0.8093
	Statistical (total)	0.0060	0.0002	0.0008	0.0008	0.0060	0.0207	0.0198	-	0.0195	0.0204	0.0260
	Sea π mass	0.0014	<0.0001	0.0002	0.0002	0.0011	0.0009	0.0006	-	0.0011	0.0008	0.0004
	Sea η_s mass	0.0024	<0.0001	<0.0001	<0.0001	0.0006	0.0019	0.0018	-	0.0019	0.0015	0.0012
	Lattice spacing	0.0009	<0.0001	<0.0001	<0.0001	0.0010	0.0015	0.0011	-	0.0011	0.0014	0.0017
	2-point function	0.0053	0.0002	0.0008	0.0008	0.0058	0.0205	0.0197	-	0.0194	0.0203	0.0259

Continued on next page

	m_H	$\sigma_{\pi H}^{\text{val}}$	$\sigma_{\pi H}^{\text{sea}}$	$\sigma_{\pi H}$	σ_{sH}^{val}	σ_{sH}^{sea}	σ_{sH}	σ_{cH}^{val}	σ_H	$\langle H_a \rangle_H$	$\langle H_a^g \rangle_H$
Systematic (total)	0.0072	0.0005	0.0007	0.0012	0.0018	0.0050	0.0050	-	0.0058	0.0128	0.0145
Scale setting	0.0037	<0.0001	<0.0001	<0.0001	0.0017	0.0002	0.0019	-	0.0019	0.0055	0.0061
fit ansatz	0.0062	0.0005	0.0007	0.0012	0.0005	0.0048	0.0043	-	0.0053	0.0114	0.0130
Sea quark correction	-	-	<0.0001	<0.0001	-	0.0015	0.0015	-	0.0015	0.0015	0.0020
Δ Central value	1.2732	0.0154	0.0272	0.0426	0	0.1018	0.1018	-	0.1444	1.1287	1.0861
Statistical (total)	0.0164	0.0026	0.0064	0.0069	0	0.0426	0.0426	-	0.0474	0.0501	0.0635
Sea π mass	0.0033	0.0001	0.0002	0.0002	0	0.0020	0.0020	-	0.0024	0.0041	0.0046
Sea η_s mass	0.0045	0.0001	0.0003	0.0003	0	0.0015	0.0015	-	0.0020	0.0040	0.0037
Lattice spacing	0.0034	<0.0001	0.0002	0.0001	0	0.0012	0.0012	-	0.0013	0.0032	0.0030
2-point function	0.0150	0.0026	0.0064	0.0069	0	0.0425	0.0425	-	0.0473	0.0497	0.0632
Systematic (total)	0.0085	0.0008	0.0010	0.0018	0	0.0030	0.0030	-	0.0048	0.0120	0.0132
Scale setting	0.0070	<0.0001	0.0001	0.0002	0	<0.0001	<0.0001	-	0.0002	0.0072	0.0072
fit ansatz	0.0049	0.0008	0.0010	0.0018	0	0.0030	0.0030	-	0.0048	0.0096	0.0111
Sea quark correction	-	-	0	0	-	0	0	-	0	0	0
Σ^* Central value	1.4172	0.0089	0.0198	0.0287	0.0949	0.0552	0.1501	-	0.1783	1.2390	1.1864
Statistical (total)	0.0128	0.0004	0.0016	0.0017	0.0050	0.0253	0.0248	-	0.0245	0.0276	0.0342
Sea π mass	0.0024	<0.0001	0.0002	0.0002	0.0002	0.0040	0.0040	-	0.0040	0.0032	0.0046
Sea η_s mass	0.0036	<0.0001	0.0001	0.0001	0.0004	0.0023	0.0024	-	0.0024	0.0027	0.0019
Lattice spacing	0.0017	<0.0001	0.0001	0.0001	0.0006	0.0012	0.0014	-	0.0014	0.0021	0.0024
2-point function	0.0119	0.0004	0.0016	0.0017	0.0049	0.0248	0.0243	-	0.0240	0.0272	0.0337
Systematic (total)	0.0204	0.0013	0.0036	0.0049	0.0005	0.0115	0.0115	-	0.0174	0.0374	0.0425
Scale setting	0.0066	<0.0001	<0.0001	0.0001	0.0005	0.0001	0.0004	-	0.0005	0.0071	0.0072
fit ansatz	0.0193	0.0013	0.0036	0.0049	<0.0001	0.0115	0.0115	-	0.0174	0.0367	0.0418
Sea quark correction	-	-	<0.0001	<0.0001	-	0.0005	0.0005	-	0.0005	0.0005	0.0006
Ξ^* Central value	1.5287	0.0048	0.0184	0.0232	0.2376	0.0741	0.3117	-	0.3346	1.1941	1.0954
Statistical (total)	0.0089	0.0002	0.0013	0.0013	0.0078	0.0231	0.0217	-	0.0215	0.0232	0.0292
Sea π mass	0.0021	<0.0001	<0.0001	<0.0001	0.0010	0.0030	0.0028	-	0.0030	0.0021	0.0032
Sea η_s mass	0.0037	<0.0001	<0.0001	<0.0001	0.0006	0.0016	0.0014	-	0.0015	0.0033	0.0031
Lattice spacing	0.0013	<0.0001	<0.0001	<0.0001	0.0009	0.0009	0.0006	-	0.0007	0.0013	0.0013
2-point function	0.0077	0.0002	0.0013	0.0013	0.0077	0.0228	0.0215	-	0.0212	0.0228	0.0288
Systematic (total)	0.0041	0.0001	0.0003	0.0004	0.0014	0.0021	0.0028	-	0.0032	0.0068	0.0077
Scale setting	0.0040	<0.0001	<0.0001	0.0001	0.0014	0.0004	0.0018	-	0.0020	0.0060	0.0065
fit ansatz	0.0009	<0.0001	0.0003	0.0003	<0.0001	0.0017	0.0018	-	0.0022	0.0031	0.0038
Sea quark correction	-	-	<0.0001	<0.0001	-	0.0012	0.0012	-	0.0012	0.0012	0.0015
Ω Central value	1.6604	0	0.0151	0.0151	0.3683	0.0934	0.4617	-	0.4770	1.1834	1.0426
Statistical (total)	0.0061	0	0.0007	0.0007	0.0095	0.0348	0.0334	-	0.0333	0.0339	0.0435
Sea π mass	0.0011	0	0.0002	0.0002	0.0014	0.0016	0.0014	-	0.0014	0.0008	0.0008
Sea η_s mass	0.0031	0	<0.0001	<0.0001	0.0008	0.0050	0.0049	-	0.0049	0.0038	0.0056
Lattice spacing	0.0018	0	0.0001	0.0001	0.0008	0.0026	0.0025	-	0.0027	0.0029	0.0037
2-point function	0.0049	0	0.0007	0.0007	0.0093	0.0343	0.0329	-	0.0328	0.0335	0.0430
Systematic (total)	0.0201	0	0.0064	0.0064	0.0022	0.0501	0.0503	-	0.0561	0.0762	0.0928
Scale setting	0.0031	0	<0.0001	<0.0001	0.0022	0.0011	0.0033	-	0.0033	0.0064	0.0074
fit ansatz	0.0199	0	0.0064	0.0064	<0.0001	0.0501	0.0502	-	0.0560	0.0759	0.0924
Sea quark correction	-	-	0.0001	0.0001	-	0.0018	0.0018	-	0.0018	0.0018	0.0024
Λ_c Central value	2.2729	0.0129	0.0133	0.0262	0	0.0597	0.0597	1.0759	1.1507	1.1223	0.7828
Statistical (total)	0.0163	0.0006	0.0015	0.0016	0	0.0234	0.0234	0.0140	0.0256	0.0254	0.0322
Sea π mass	0.0021	<0.0001	0.0002	0.0002	0	0.0015	<0.0001	0.0018	0.0042	0.0040	0.0052
Sea η_s mass	0.0035	<0.0001	0.0001	0.0001	0	0.0017	0.0005	0.0017	0.0027	0.0037	0.0041
Lattice spacing	0.0030	0.0001	0.0002	<0.0001	0	0.0007	0.0006	0.0016	0.0054	0.0054	0.0070
2-point function	0.0155	0.0006	0.0015	0.0016	0	0.0233	0.0234	0.0137	0.0245	0.0242	0.0307

Continued on next page

	m_H	$\sigma_{\pi H}^{\text{val}}$	$\sigma_{\pi H}^{\text{sea}}$	$\sigma_{\pi H}$	σ_{sH}^{val}	σ_{sH}^{sea}	σ_{sH}	σ_{cH}^{val}	σ_H	$\langle H_a \rangle_H$	$\langle H_a^g \rangle_H$
Systematic (total)	0.0164	0.0004	0.0012	0.0015	0	0.0062	0.0062	0.0029	0.0080	0.0247	0.0271
Scale setting	0.0081	<0.0001	0.0002	0.0003	0	0.0004	0.0004	0.0026	0.0019	0.0101	0.0106
D_s mass	0.0009	<0.0001	0.0001	<0.0001	0	0.0006	0.0006	0.0013	0.0005	0.0015	0.0016
fit ansatz	0.0142	0.0003	0.0011	0.0015	0	0.0058	0.0058	0.0002	0.0075	0.0224	0.0247
Sea quark correction	-	-	0.0002	0.0002	-	0.0020	0.0020	-	0.0020	0.0020	0.0026
Σ_c Central value	2.4574	0.0093	0.0132	0.0225	0	0.0316	0.0316	1.1071	1.1493	1.3086	0.9696
Statistical (total)	0.0201	0.0008	0.0019	0.0021	0	0.0299	0.0298	0.0296	0.0271	0.0280	0.0352
Sea π mass	0.0025	<0.0001	0.0002	0.0002	0	0.0050	0.0009	0.0010	0.0034	0.0023	0.0035
Sea η_s mass	0.0022	<0.0001	<0.0001	0.0001	0	0.0017	<0.0001	0.0024	0.0015	0.0035	0.0038
Lattice spacing	0.0044	<0.0001	0.0002	0.0002	0	0.0009	0.0009	0.0013	0.0011	0.0026	0.0025
2-point function	0.0193	0.0008	0.0019	0.0021	0	0.0294	0.0298	0.0295	0.0268	0.0276	0.0347
Systematic (total)	0.0197	0.0009	0.0011	0.0020	0	0.0042	0.0042	0.0010	0.0057	0.0251	0.0267
Scale setting	0.0048	<0.0001	<0.0001	<0.0001	0	0.0009	0.0009	0.0006	0.0003	0.0045	0.0044
D_s mass	0.0018	<0.0001	<0.0001	<0.0001	0	0.0014	0.0014	0.0007	0.0003	0.0022	0.0023
fit ansatz	0.0190	0.0009	0.0011	0.0020	0	0.0033	0.0033	0.0003	0.0053	0.0245	0.0261
Sea quark correction	-	-	0.0002	0.0002	-	0.0020	0.0020	-	0.0020	0.0020	0.0026
Ξ_c Central value	2.4762	0.0060	0.0082	0.0142	0.1546	0.0573	0.2119	1.0680	1.2981	1.1777	0.7948
Statistical (total)	0.0126	0.0002	0.0010	0.0011	0.0079	0.0178	0.0195	0.0077	0.0187	0.0207	0.0256
Sea π mass	0.0007	<0.0001	<0.0001	0.0001	0.0003	0.0006	0.0002	0.0008	0.0018	0.0028	0.0034
Sea η_s mass	0.0031	<0.0001	<0.0001	<0.0001	0.0008	0.0010	0.0002	0.0013	0.0023	0.0045	0.0051
Lattice spacing	0.0017	<0.0001	<0.0001	<0.0001	0.0003	0.0003	<0.0001	0.0009	0.0006	0.0025	0.0028
2-point function	0.0121	0.0002	0.0010	0.0011	0.0078	0.0178	0.0195	0.0075	0.0185	0.0199	0.0247
Systematic (total)	0.0043	0.0001	0.0003	0.0003	0.0005	0.0021	0.0022	0.0023	0.0038	0.0071	0.0081
Scale setting	0.0038	<0.0001	<0.0001	0.0001	0.0005	<0.0001	0.0005	0.0019	0.0028	0.0065	0.0073
D_s mass	0.0010	<0.0001	<0.0001	<0.0001	<0.0001	0.0002	0.0002	0.0013	0.0016	0.0005	0.0010
fit ansatz	0.0018	<0.0001	0.0001	0.0002	<0.0001	0.0002	0.0001	<0.0001	0.0003	0.0019	0.0020
Sea quark correction	-	-	0.0002	0.0002	-	0.0021	0.0021	-	0.0021	0.0021	0.0027
Ξ'_c Central value	2.5726	0.0047	0.0110	0.0157	0.1391	0.0764	0.2155	1.0844	1.3222	1.2500	0.8600
Statistical (total)	0.0141	0.0003	0.0012	0.0013	0.0155	0.0207	0.0224	0.0083	0.0209	0.0230	0.0285
Sea π mass	0.0020	<0.0001	<0.0001	<0.0001	0.0067	0.0028	0.0003	0.0032	0.0080	0.0062	0.0086
Sea η_s mass	0.0043	<0.0001	0.0001	0.0002	0.0071	0.0019	0.0007	0.0016	0.0065	0.0068	0.0086
Lattice spacing	0.0013	<0.0001	0.0002	0.0002	0.0078	0.0011	0.0003	0.0012	0.0064	0.0049	0.0069
2-point function	0.0132	0.0003	0.0012	0.0013	0.0091	0.0204	0.0224	0.0074	0.0170	0.0205	0.0248
Systematic (total)	0.0071	0.0003	0.0005	0.0008	0.0009	0.0068	0.0070	0.0024	0.0085	0.0139	0.0163
Scale setting	0.0048	<0.0001	<0.0001	<0.0001	0.0009	<0.0001	0.0010	0.0016	0.0022	0.0070	0.0076
D_s mass	0.0035	<0.0001	<0.0001	0.0001	0.0001	0.0005	0.0003	0.0016	0.0009	0.0027	0.0024
fit ansatz	0.0039	0.0003	0.0005	0.0008	<0.0001	0.0065	0.0065	0.0007	0.0079	0.0116	0.0139
Sea quark correction	-	-	0.0002	0.0002	-	0.0021	0.0021	-	0.0021	0.0021	0.0027
Ω_c Central value	2.6985	0	0.0115	0.0115	0.2505	0.0434	0.2939	1.0865	1.3924	1.3128	0.9025
Statistical (total)	0.0123	0	0.0019	0.0019	0.0101	0.0244	0.0222	0.0067	0.0235	0.0260	0.0321
Sea π mass	0.0009	0	<0.0001	<0.0001	0.0002	<0.0001	0.0015	0.0005	0.0013	0.0014	0.0014
Sea η_s mass	0.0021	0	<0.0001	<0.0001	0.0006	0.0001	0.0014	0.0010	0.0019	0.0038	0.0043
Lattice spacing	0.0016	0	<0.0001	<0.0001	0.0011	0.0003	0.0015	0.0010	0.0004	0.0031	0.0034
2-point function	0.0120	0	0.0019	0.0019	0.0100	0.0244	0.0221	0.0065	0.0234	0.0255	0.0316
Systematic (total)	0.0038	0	0.0003	0.0003	0.0005	0.0025	0.0024	0.0018	0.0029	0.0030	0.0034
Scale setting	0.0035	0	<0.0001	<0.0001	0.0005	0.0007	0.0002	0.0013	0.0014	0.0017	0.0013
D_s mass	0.0013	0	<0.0001	<0.0001	<0.0001	<0.0001	<0.0001	0.0012	0.0008	0.0006	0.0004
fit ansatz	0.0008	0	0.0002	0.0002	<0.0001	0.0003	0.0003	<0.0001	0.0005	0.0005	0.0006
Sea quark correction	-	-	0.0002	0.0002	-	0.0023	0.0023	-	0.0024	0.0024	0.0031
Σ_c^* Central value	2.5320	0.0083	0.0209	0.0291	0	0.0389	0.0389	1.0551	1.1201	1.4114	1.0810

Continued on next page

	m_H	$\sigma_{\pi H}^{\text{val}}$	$\sigma_{\pi H}^{\text{sea}}$	$\sigma_{\pi H}$	σ_{sH}^{val}	σ_{sH}^{sea}	σ_{sH}	σ_{cH}^{val}	σ_H	$\langle H_a \rangle_H$	$\langle H_a^g \rangle_H$
Statistical (total)	0.0262	0.0016	0.0027	0.0034	0	0.0429	0.0429	0.0125	0.0281	0.0310	0.0386
Sea π mass	0.0055	0.0002	<0.0001	0.0001	0	0.0024	0.0002	0.0013	0.0026	0.0035	0.0046
Sea η_s mass	0.0022	0.0001	0.0002	0.0002	0	0.0009	0.0001	0.0014	0.0024	0.0024	0.0031
Lattice spacing	0.0073	<0.0001	0.0002	0.0003	0	0.0009	0.0001	0.0011	0.0021	0.0046	0.0046
2-point function	0.0245	0.0016	0.0027	0.0034	0	0.0428	0.0429	0.0123	0.0278	0.0304	0.0379
Systematic (total)	0.0555	0.0016	0.0054	0.0070	0	0.0208	0.0208	0.0018	0.0281	0.0830	0.0912
Scale setting	0.0026	<0.0001	0.0001	0.0002	0	0.0009	0.0009	0.0015	0.0021	0.0047	0.0053
D_s mass	0.0004	<0.0001	<0.0001	<0.0001	0	0.0003	0.0003	0.0010	0.0009	0.0005	0.0007
fit ansatz	0.0554	0.0016	0.0054	0.0070	0	0.0207	0.0207	0.0002	0.0279	0.0829	0.0910
Sea quark correction	-	-	0.0002	0.0002	-	0.0019	0.0019	-	0.0019	0.0019	0.0025
Ξ_c^* Central value	2.6460	0.0044	0.0134	0.0178	0.1247	0.0621	0.1868	1.0331	1.2432	1.4027	1.0359
Statistical (total)	0.0158	0.0002	0.0012	0.0013	0.0081	0.0222	0.0237	0.0073	0.0206	0.0240	0.0292
Sea π mass	0.0012	<0.0001	<0.0001	0.0001	0.0004	0.0024	0.0004	0.0007	0.0022	0.0031	0.0037
Sea η_s mass	0.0042	<0.0001	<0.0001	<0.0001	0.0011	0.0009	0.0003	0.0013	0.0023	0.0016	0.0015
Lattice spacing	0.0029	<0.0001	0.0001	0.0002	0.0010	0.0009	0.0002	0.0015	0.0028	0.0053	0.0062
2-point function	0.0149	0.0002	0.0012	0.0013	0.0080	0.0220	0.0237	0.0070	0.0202	0.0231	0.0283
Systematic (total)	0.0083	0.0001	0.0005	0.0006	0.0007	0.0030	0.0032	0.0019	0.0047	0.0123	0.0136
Scale setting	0.0045	<0.0001	<0.0001	0.0001	0.0007	0.0008	0.0015	0.0015	0.0031	0.0075	0.0085
D_s mass	0.0010	<0.0001	<0.0001	<0.0001	<0.0001	0.0001	0.0002	0.0012	0.0013	0.0003	0.0006
fit ansatz	0.0069	0.0001	0.0005	0.0006	<0.0001	0.0021	0.0021	0.0001	0.0027	0.0096	0.0103
Sea quark correction	-	-	0.0002	0.0002	-	0.0020	0.0020	-	0.0020	0.0020	0.0026
Ω_c^* Central value	2.7801	0	0.0129	0.0129	0.2431	0.0766	0.3197	1.0464	1.3811	1.4052	0.9984
Statistical (total)	0.0134	0	0.0019	0.0019	0.0099	0.0212	0.0188	0.0062	0.0205	0.0260	0.0314
Sea π mass	0.0004	0	0.0001	0.0001	0.0012	<0.0001	0.0017	0.0004	0.0023	0.0036	0.0043
Sea η_s mass	0.0024	0	<0.0001	<0.0001	0.0012	<0.0001	0.0004	0.0012	0.0007	0.0032	0.0035
Lattice spacing	0.0021	0	<0.0001	<0.0001	0.0003	0.0004	0.0011	0.0014	0.0026	0.0044	0.0052
2-point function	0.0130	0	0.0019	0.0019	0.0097	0.0212	0.0187	0.0059	0.0202	0.0252	0.0305
Systematic (total)	0.0040	0	0.0004	0.0004	0.0008	0.0031	0.0032	0.0023	0.0046	0.0073	0.0085
Scale setting	0.0036	0	<0.0001	<0.0001	0.0008	0.0002	0.0010	0.0020	0.0029	0.0066	0.0074
D_s mass	0.0014	0	<0.0001	<0.0001	<0.0001	0.0002	0.0002	0.0012	0.0013	0.0001	0.0003
fit ansatz	0.0010	0	0.0003	0.0003	<0.0001	0.0021	0.0021	<0.0001	0.0024	0.0022	0.0030
Sea quark correction	-	-	0.0002	0.0002	-	0.0023	0.0023	-	0.0023	0.0023	0.0029
Ξ_{cc} Central value	3.6358	0.0044	0.0067	0.0111	0	0.0741	0.0741	2.1305	2.2156	1.4201	0.7665
Statistical (total)	0.0145	0.0004	0.0014	0.0015	0	0.0203	0.0203	0.0287	0.0340	0.0337	0.0432
Sea π mass	0.0008	<0.0001	<0.0001	0.0001	0	0.0006	0.0002	0.0062	0.0063	0.0070	0.0089
Sea η_s mass	0.0023	<0.0001	0.0001	0.0001	0	0.0013	0.0003	0.0061	0.0056	0.0049	0.0064
Lattice spacing	0.0007	<0.0001	<0.0001	<0.0001	0	0.0015	<0.0001	0.0018	0.0010	0.0036	0.0041
2-point function	0.0143	0.0004	0.0014	0.0015	0	0.0202	0.0203	0.0273	0.0329	0.0324	0.0416
Systematic (total)	0.0161	0.0012	0.0007	0.0018	0	0.0232	0.0232	0.0052	0.0258	0.0414	0.0490
Scale setting	0.0011	<0.0001	<0.0001	<0.0001	0	0.0003	0.0003	0.0044	0.0045	0.0055	0.0068
D_s mass	0.0021	<0.0001	<0.0001	<0.0001	0	0.0001	0.0001	0.0027	0.0026	0.0005	0.0012
fit ansatz	0.0159	0.0012	0.0005	0.0017	0	0.0229	0.0229	0.0005	0.0249	0.0409	0.0483
Sea quark correction	-	-	0.0004	0.0004	-	0.0039	0.0039	-	0.0039	0.0039	0.0051
Ω_{cc} Central value	3.7287	0	0.0083	0.0083	0.1187	0.0382	0.1569	2.0996	2.2629	1.4704	0.8031
Statistical (total)	0.0119	0	0.0013	0.0013	0.0075	0.0159	0.0141	0.0129	0.0185	0.0233	0.0284
Sea π mass	0.0007	0	<0.0001	<0.0001	0.0004	0.0002	0.0018	0.0022	0.0037	0.0048	0.0058
Sea η_s mass	0.0007	0	<0.0001	<0.0001	0.0006	0.0002	0.0016	0.0026	0.0023	0.0040	0.0045
Lattice spacing	0.0006	0	<0.0001	<0.0001	0.0007	0.0001	0.0011	0.0026	0.0035	0.0042	0.0051
2-point function	0.0118	0	0.0013	0.0013	0.0074	0.0159	0.0138	0.0122	0.0176	0.0220	0.0269
Systematic (total)	0.0034	0	0.0004	0.0004	0.0009	0.0041	0.0039	0.0038	0.0057	0.0076	0.0089

Continued on next page

	m_H	$\sigma_{\pi H}^{\text{val}}$	$\sigma_{\pi H}^{\text{sea}}$	$\sigma_{\pi H}$	σ_{sH}^{val}	σ_{sH}^{sea}	σ_{sH}	σ_{cH}^{val}	σ_H	$\langle H_a \rangle_H$	$\langle H_a^g \rangle_H$
Scale setting	0.0015	0	<0.0001	<0.0001	0.0009	0.0011	0.0003	0.0031	0.0035	0.0065	0.0073
D_s mass	0.0030	0	<0.0001	<0.0001	<0.0001	0.0002	0.0002	0.0023	0.0022	0.0003	0.0004
fit ansatz	<0.0001	0	<0.0001	<0.0001	0.0001	0.0003	0.0002	0.0002	<0.0001	<0.0001	<0.0001
Sea quark correction	-	-	0.0004	0.0004	-	0.0039	0.0039	-	0.0039	0.0039	0.0051
Ξ_{cc}^* Central value	3.7097	0.0038	0.0071	0.0110	0	0.1057	0.1057	2.0237	2.1387	1.5707	0.9398
Statistical (total)	0.0157	0.0005	0.0015	0.0017	0	0.0206	0.0206	0.0238	0.0337	0.0348	0.0439
Sea π mass	0.0009	<0.0001	<0.0001	<0.0001	0	0.0008	<0.0001	0.0057	0.0056	0.0043	0.0059
Sea η_s mass	0.0030	<0.0001	<0.0001	<0.0001	0	0.0015	0.0002	0.0028	0.0018	0.0060	0.0069
Lattice spacing	0.0032	<0.0001	<0.0001	<0.0001	0	0.0009	0.0002	0.0051	0.0031	0.0052	0.0059
2-point function	0.0150	0.0005	0.0015	0.0017	0	0.0205	0.0206	0.0224	0.0330	0.0336	0.0425
Systematic (total)	0.0035	0.0000	0.0004	0.0004	0	0.0047	0.0047	0.0063	0.0091	0.0112	0.0138
Scale setting	0.0024	<0.0001	<0.0001	0.0001	0	0.0005	0.0005	0.0055	0.0069	0.0094	0.0114
D_s mass	0.0022	<0.0001	<0.0001	<0.0001	0	0.0001	0.0001	0.0030	0.0028	0.0006	0.0014
fit ansatz	0.0014	<0.0001	<0.0001	<0.0001	0	0.0028	0.0028	0.0005	0.0036	0.0047	0.0058
Sea quark correction	-	-	0.0004	0.0004	-	0.0037	0.0037	-	0.0037	0.0037	0.0048
Ω_{cc}^* Central value	3.8265	0	0.0062	0.0062	0.1073	0.0461	0.1534	2.0428	2.1985	1.6192	0.9711
Statistical (total)	0.0107	0	0.0012	0.0012	0.0061	0.0160	0.0148	0.0137	0.0184	0.0219	0.0267
Sea π mass	0.0012	0	<0.0001	<0.0001	0.0003	<0.0001	0.0004	0.0018	0.0022	0.0032	0.0038
Sea η_s mass	0.0009	0	<0.0001	<0.0001	0.0002	<0.0001	0.0006	0.0047	0.0029	0.0040	0.0049
Lattice spacing	0.0010	0	<0.0001	<0.0001	0.0005	<0.0001	0.0006	0.0033	0.0039	0.0048	0.0059
2-point function	0.0105	0	0.0012	0.0012	0.0061	0.0160	0.0148	0.0123	0.0176	0.0208	0.0253
Systematic (total)	0.0037	0	0.0004	0.0004	0.0002	0.0039	0.0039	0.0059	0.0060	0.0074	0.0090
Scale setting	0.0025	0	<0.0001	<0.0001	0.0002	0.0008	0.0006	0.0054	0.0042	0.0063	0.0075
D_s mass	0.0027	0	<0.0001	<0.0001	<0.0001	0.0003	0.0003	0.0024	0.0022	0.0005	0.0001
fit ansatz	0.0004	0	<0.0001	<0.0001	<0.0001	0.0005	0.0005	0.0002	<0.0001	0.0002	0.0002
Sea quark correction	-	-	0.0004	0.0004	-	0.0038	0.0038	-	0.0038	0.0038	0.0049
Ω_{ccc} Central value	4.8123	0	0.0071	0.0071	0	0.0446	0.0446	2.9773	3.0276	1.7841	0.8911
Statistical (total)	0.0084	0	0.0010	0.0010	0	0.0081	0.0081	0.0164	0.0166	0.0183	0.0229
Sea π mass	0.0008	0	<0.0001	<0.0001	0	0.0001	0.0007	0.0032	0.0021	0.0023	0.0029
Sea η_s mass	0.0006	0	<0.0001	<0.0001	0	<0.0001	0.0001	0.0050	0.0034	0.0030	0.0041
Lattice spacing	0.0004	0	<0.0001	<0.0001	0	<0.0001	0.0003	0.0042	0.0038	0.0039	0.0050
2-point function	0.0083	0	0.0010	0.0010	0	0.0081	0.0081	0.0147	0.0156	0.0175	0.0218
Systematic (total)	0.0041	0	0.0006	0.0006	0	0.0055	0.0055	0.0064	0.0085	0.0091	0.0114
Scale setting	0.0011	0	<0.0001	<0.0001	0	0.0003	0.0003	0.0053	0.0054	0.0071	0.0087
D_s mass	0.0039	0	<0.0001	<0.0001	0	0.0001	0.0001	0.0035	0.0035	0.0001	0.0009
fit ansatz	0.0002	0	<0.0001	<0.0001	0	0.0002	0.0002	0.0011	0.0007	0.0018	0.0020
Sea quark correction	-	-	0.0006	0.0006	-	0.0054	0.0054	-	0.0055	0.0055	0.0071
D Central value	1.8662	0.0039	0.0042	0.0081	0	0.0223	0.0223	1.1450	1.1748	0.6914	0.3448
Statistical (total)	0.0032	0.0001	0.0003	0.0003	0	0.0054	0.0054	0.0036	0.0053	0.0053	0.0067
Sea π mass	0.0005	<0.0001	<0.0001	<0.0001	0	0.0003	<0.0001	0.0002	0.0006	<0.0001	0.0004
Sea η_s mass	0.0002	<0.0001	<0.0001	<0.0001	0	0.0002	<0.0001	0.0007	0.0008	0.0010	0.0012
Lattice spacing	0.0007	<0.0001	<0.0001	<0.0001	0	0.0002	<0.0001	0.0006	0.0004	0.0009	0.0011
2-point function	0.0031	0.0001	0.0003	0.0003	0	0.0054	0.0054	0.0035	0.0052	0.0051	0.0065
Systematic (total)	0.0047	0.0002	0.0003	0.0005	0	0.0021	0.0021	0.0014	0.0026	0.0049	0.0053
Scale setting	0.0003	<0.0001	<0.0001	<0.0001	0	<0.0001	<0.0001	0.0008	0.0009	0.0012	0.0015
D_s mass	0.0016	<0.0001	<0.0001	<0.0001	0	<0.0001	<0.0001	0.0011	0.0012	0.0004	<0.0001
fit ansatz	0.0044	0.0002	0.0002	0.0004	0	0.0004	0.0004	<0.0001	<0.0001	0.0043	0.0043
Sea quark correction	-	-	0.0002	0.0002	-	0.0021	0.0021	-	0.0021	0.0021	0.0027
D^* Central value	2.0088	0.0037	0.0067	0.0104	0	0.0317	0.0317	1.0530	1.0954	0.9133	0.5901
Statistical (total)	0.0065	0.0002	0.0005	0.0005	0	0.0083	0.0084	0.0043	0.0073	0.0088	0.0106

Continued on next page

	m_H	$\sigma_{\pi H}^{\text{val}}$	$\sigma_{\pi H}^{\text{sea}}$	$\sigma_{\pi H}$	σ_{sH}^{val}	σ_{sH}^{sea}	σ_{sH}	σ_{cH}^{val}	σ_H	$\langle H_a \rangle_H$	$\langle H_a^g \rangle_H$
Sea π mass	0.0009	<0.0001	<0.0001	<0.0001	0	0.0003	0.0003	0.0007	0.0003	0.0007	0.0007
Sea η_s mass	0.0014	<0.0001	<0.0001	<0.0001	0	0.0007	0.0002	0.0015	0.0011	0.0019	0.0022
Lattice spacing	0.0020	<0.0001	<0.0001	<0.0001	0	0.0004	0.0002	0.0012	0.0010	0.0023	0.0026
2-point function	0.0060	0.0002	0.0005	0.0005	0	0.0083	0.0084	0.0038	0.0071	0.0082	0.0100
Systematic (total)	0.0069	0.0002	0.0004	0.0006	0	0.0020	0.0020	0.0020	0.0029	0.0086	0.0092
Scale setting	0.0023	<0.0001	<0.0001	<0.0001	0	<0.0001	<0.0001	0.0017	0.0016	0.0039	0.0044
D_s mass	0.0018	<0.0001	<0.0001	<0.0001	0	<0.0001	<0.0001	0.0010	0.0010	0.0008	0.0005
fit ansatz	0.0062	0.0002	0.0004	0.0005	0	0.0006	0.0006	<0.0001	0.0011	0.0074	0.0077
Sea quark correction	-	-	0.0002	0.0002	-	0.0019	0.0019	-	0.0019	0.0019	0.0025
D_s Central value	1.9667	0	0.0037	0.0037	0.1039	0.0231	0.1270	1.1371	1.2685	0.6982	0.3240
Statistical (total)	0	0	0	0	0.0018	0	0.0018	0.0046	0.0048	0.0048	0.0061
Sea π mass	0	0	0	0	0.0004	0	0.0004	0.0008	0.0004	0.0004	0.0005
Sea η_s mass	0	0	0	0	<0.0001	0	<0.0001	0.0011	0.0011	0.0011	0.0014
Lattice spacing	0	0	0	0	0.0001	0	0.0001	0.0022	0.0021	0.0021	0.0027
2-point function	0	0	0	0	0.0018	0	0.0018	0.0038	0.0041	0.0041	0.0053
Systematic (total)	0.0015	0	0.0002	0.0002	0.0003	0.0021	0.0022	0.0035	0.0039	0.0037	0.0047
Scale setting	0	0	0	0	0.0003	0	0.0003	0.0033	0.0030	0.0030	0.0038
D_s mass	0.0015	0	0	0	<0.0001	0	<0.0001	0.0011	0.0012	0.0003	<0.0001
fit ansatz	0	0	0	0	<0.0001	0	<0.0001	<0.0001	0.0001	0.0001	0.0002
Sea quark correction	-	-	0.0002	0.0002	-	0.0021	0.0021	-	0.0022	0.0022	0.0028
D_s^* Central value	2.1142	0	0.0053	0.0053	0.1042	0.0326	0.1367	1.0455	1.1874	0.9274	0.5773
Statistical (total)	0.0035	0	0.0005	0.0005	0.0043	0.0066	0.0050	0.0037	0.0062	0.0086	0.0103
Sea π mass	0.0004	0	<0.0001	<0.0001	0.0005	<0.0001	0.0001	0.0002	0.0007	0.0002	0.0006
Sea η_s mass	0.0006	0	<0.0001	<0.0001	0.0005	<0.0001	0.0001	0.0013	0.0014	0.0020	0.0024
Lattice spacing	0.0007	0	<0.0001	<0.0001	0.0003	<0.0001	0.0002	0.0011	0.0012	0.0018	0.0022
2-point function	0.0034	0	0.0005	0.0005	0.0042	0.0066	0.0050	0.0033	0.0059	0.0082	0.0098
Systematic (total)	0.0021	0	0.0002	0.0002	0.0002	0.0020	0.0020	0.0022	0.0032	0.0044	0.0053
Scale setting	0.0016	0	<0.0001	<0.0001	0.0002	<0.0001	0.0003	0.0018	0.0022	0.0039	0.0045
D_s mass	0.0013	0	<0.0001	<0.0001	<0.0001	<0.0001	<0.0001	0.0011	0.0012	0.0001	0.0002
fit ansatz	0.0002	0	<0.0001	<0.0001	<0.0001	0.0004	0.0004	<0.0001	0.0004	0.0005	0.0006
Sea quark correction	-	-	0.0002	0.0002	-	0.0020	0.0020	-	0.0020	0.0020	0.0026
η_c Central value	2.9758	0	0.0024	0.0024	0	0.0193	0.0193	2.0580	2.0793	0.8971	0.2836
Statistical (total)	0.0034	0	0.0004	0.0004	0	0.0039	0.0038	0.0050	0.0062	0.0049	0.0063
Sea π mass	0.0004	0	<0.0001	<0.0001	0	<0.0001	0.0005	0.0007	0.0009	0.0007	0.0010
Sea η_s mass	0.0004	0	<0.0001	<0.0001	0	<0.0001	0.0003	0.0018	0.0022	0.0016	0.0022
Lattice spacing	0.0010	0	<0.0001	<0.0001	0	<0.0001	0.0002	0.0022	0.0021	0.0011	0.0017
2-point function	0.0032	0	0.0004	0.0004	0	0.0039	0.0038	0.0040	0.0053	0.0044	0.0056
Systematic (total)	0.0030	0	0.0004	0.0004	0	0.0038	0.0038	0.0036	0.0050	0.0041	0.0054
Scale setting	0.0012	0	<0.0001	<0.0001	0	0.0002	0.0002	0.0028	0.0026	0.0015	0.0022
D_s mass	0.0028	0	<0.0001	<0.0001	0	<0.0001	<0.0001	0.0022	0.0021	0.0006	<0.0001
fit ansatz	<0.0001	0	<0.0001	<0.0001	0	<0.0001	<0.0001	<0.0001	0.0001	<0.0001	<0.0001
Sea quark correction	-	-	0.0004	0.0004	-	0.0038	0.0038	-	0.0038	0.0038	0.0049
J/ψ Central value	3.0918	0	0.0031	0.0031	0	0.0253	0.0253	1.9932	2.0214	1.0723	0.4760
Statistical (total)	0.0032	0	0.0004	0.0004	0	0.0036	0.0036	0.0055	0.0065	0.0061	0.0078
Sea π mass	0.0003	0	<0.0001	<0.0001	0	<0.0001	0.0003	0.0015	0.0007	0.0007	0.0007
Sea η_s mass	0.0003	0	<0.0001	<0.0001	0	<0.0001	0.0002	0.0028	0.0027	0.0022	0.0030
Lattice spacing	0.0003	0	<0.0001	<0.0001	0	<0.0001	0.0002	0.0023	0.0025	0.0023	0.0031
2-point function	0.0032	0	0.0004	0.0004	0	0.0036	0.0036	0.0039	0.0053	0.0051	0.0064
Systematic (total)	0.0026	0	0.0004	0.0004	0	0.0037	0.0037	0.0040	0.0052	0.0048	0.0062
Scale setting	<0.0001	0	<0.0001	<0.0001	0	0.0003	0.0003	0.0034	0.0031	0.0031	0.0040

Continued on next page

	m_H	$\sigma_{\pi H}^{\text{val}}$	$\sigma_{\pi H}^{\text{sea}}$	$\sigma_{\pi H}$	σ_{sH}^{val}	σ_{sH}^{sea}	σ_{sH}	σ_{cH}^{val}	σ_H	$\langle H_a \rangle_H$	$\langle H_a^g \rangle_H$
D_s mass	0.0026	0	<0.0001	<0.0001	0	<0.0001	<0.0001	0.0021	0.0021	0.0006	<0.0001
fit ansatz	<0.0001	0	<0.0001	<0.0001	0	0.0001	0.0001	0.0003	0.0004	0.0004	0.0006
Sea quark correction	-	-	0.0004	0.0004	-	0.0036	0.0036	-	0.0037	0.0037	0.0047
χ_{c0} Central value	3.3980	0	0.0073	0.0073	0	0.0757	0.0757	2.0878	2.1850	1.2281	0.5837
Statistical (total)	0.0186	0	0.0025	0.0025	0	0.0194	0.0195	0.0282	0.0308	0.0378	0.0462
Sea π mass	0.0007	0	<0.0001	<0.0001	0	0.0003	0.0007	0.0016	0.0020	0.0020	0.0026
Sea η_s mass	0.0016	0	<0.0001	<0.0001	0	0.0002	0.0014	0.0024	0.0004	0.0019	0.0021
Lattice spacing	0.0005	0	<0.0001	<0.0001	0	0.0001	0.0003	0.0024	0.0028	0.0025	0.0033
2-point function	0.0185	0	0.0025	0.0025	0	0.0194	0.0194	0.0279	0.0306	0.0376	0.0460
Systematic (total)	0.0028	0	0.0004	0.0004	0	0.0038	0.0038	0.0032	0.0049	0.0050	0.0062
Scale setting	0.0004	0	<0.0001	<0.0001	0	0.0004	0.0004	0.0024	0.0023	0.0030	0.0037
D_s mass	0.0028	0	<0.0001	<0.0001	0	<0.0001	<0.0001	0.0021	0.0020	0.0008	0.0002
fit ansatz	<0.0001	0	<0.0001	<0.0001	0	0.0002	0.0002	<0.0001	0.0004	0.0005	0.0006
Sea quark correction	-	-	0.0004	0.0004	-	0.0038	0.0038	-	0.0038	0.0038	0.0050
χ_{c1} Central value	3.5166	0	0.0058	0.0058	0	0.0552	0.0552	2.0046	2.0643	1.4668	0.8585
Statistical (total)	0.0226	0	0.0029	0.0029	0	0.0222	0.0222	0.0179	0.0279	0.0336	0.0411
Sea π mass	0.0015	0	0.0002	0.0002	0	<0.0001	0.0011	0.0008	0.0027	0.0033	0.0041
Sea η_s mass	0.0033	0	0.0001	0.0001	0	0.0003	0.0003	0.0015	0.0032	0.0047	0.0056
Lattice spacing	0.0009	0	0.0001	0.0001	0	0.0001	0.0007	0.0035	0.0029	0.0041	0.0050
2-point function	0.0223	0	0.0029	0.0029	0	0.0222	0.0222	0.0175	0.0274	0.0328	0.0402
Systematic (total)	0.0037	0	0.0004	0.0004	0	0.0037	0.0037	0.0040	0.0055	0.0069	0.0083
Scale setting	0.0021	0	<0.0001	<0.0001	0	0.0002	0.0002	0.0035	0.0035	0.0057	0.0068
D_s mass	0.0030	0	<0.0001	<0.0001	0	<0.0001	<0.0001	0.0019	0.0020	0.0012	0.0006
fit ansatz	<0.0001	0	<0.0001	<0.0001	0	0.0006	0.0006	<0.0001	0.0006	<0.0001	0.0002
Sea quark correction	-	-	0.0004	0.0004	-	0.0037	0.0037	-	0.0037	0.0037	0.0048
h_c Central value	3.5415	0	0.0109	0.0109	0	0.0404	0.0404	1.9860	2.0381	1.5223	0.9222
Statistical (total)	0.0180	0	0.0028	0.0028	0	0.0216	0.0217	0.0219	0.0290	0.0359	0.0440
Sea π mass	0.0023	0	0.0002	0.0002	0	0.0008	0.0015	0.0018	0.0031	0.0015	0.0028
Sea η_s mass	0.0018	0	<0.0001	<0.0001	0	0.0006	0.0006	0.0018	0.0030	0.0020	0.0031
Lattice spacing	0.0027	0	0.0002	0.0002	0	0.0005	0.0005	0.0041	0.0023	0.0044	0.0051
2-point function	0.0176	0	0.0028	0.0028	0	0.0216	0.0216	0.0214	0.0286	0.0355	0.0435
Systematic (total)	0.0037	0	0.0004	0.0004	0	0.0039	0.0039	0.0053	0.0070	0.0090	0.0109
Scale setting	0.0027	0	0.0001	0.0001	0	0.0009	0.0009	0.0047	0.0053	0.0082	0.0097
D_s mass	0.0025	0	<0.0001	<0.0001	0	0.0004	0.0004	0.0025	0.0027	0.0002	0.0010
fit ansatz	0.0004	0	0.0002	0.0002	0	0.0009	0.0009	0.0001	0.0010	0.0003	0.0006
Sea quark correction	-	-	0.0004	0.0004	-	0.0036	0.0036	-	0.0036	0.0036	0.0047